4-D topography – promises and pitfalls

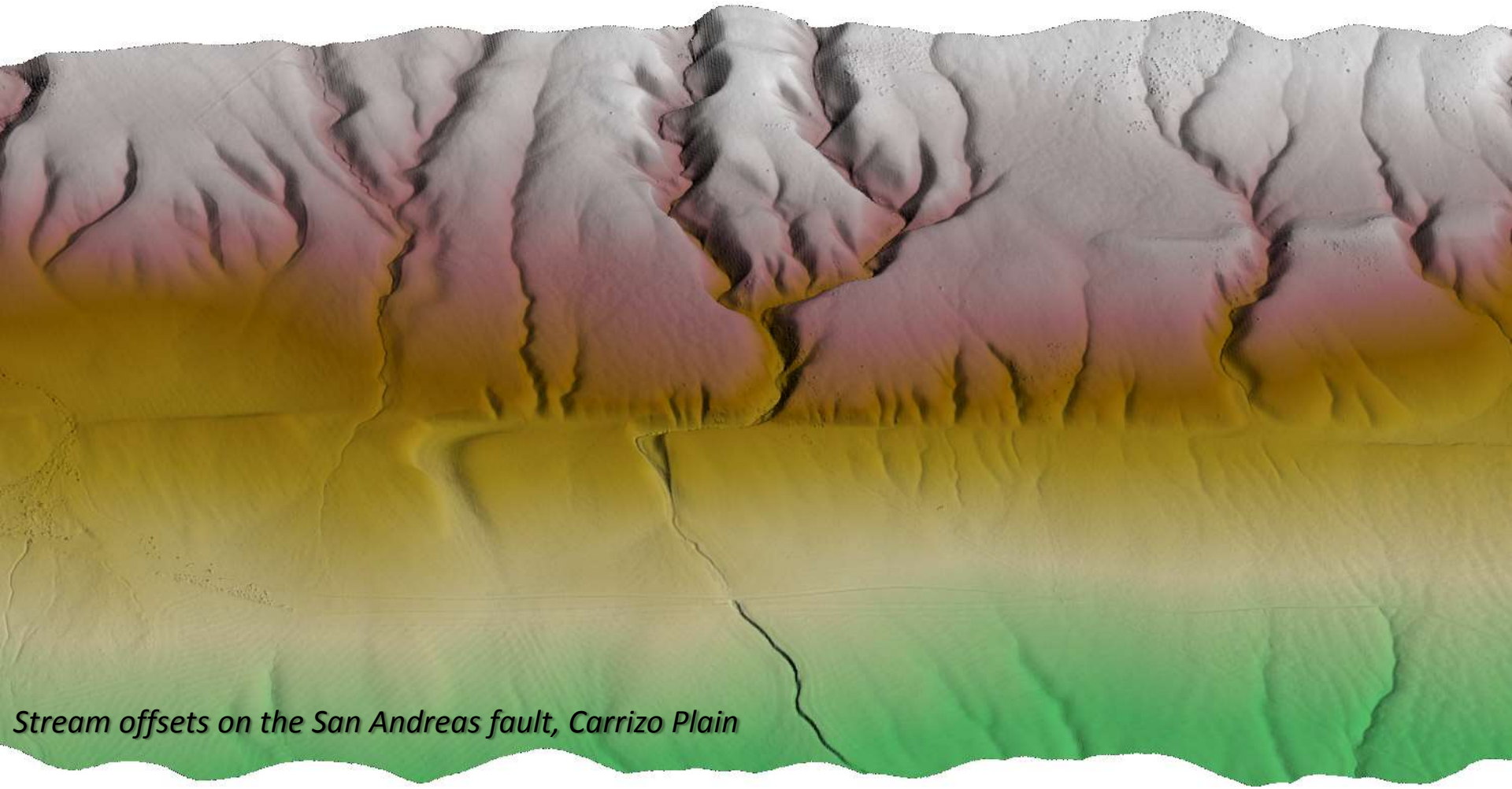

Stream offsets on the San Andreas fault, Carrizo Plain

Edwin Nissen (enissen@mines.edu)

COLORADO SCHOOL OF MINES
EARTH • ENERGY • ENVIRONMENT

SCEC
an NSF + USGS center

USGS
science for a changing world

4-D topography – promises and pitfalls

Stream offsets on the San Andreas fault, Carrizo Plain

- Importance of “seeing” at the appropriate scale

4-D topography – promises and pitfalls

How long is the coast of Britain?
Statistical self-similarity and fractional dimensio
Science: 156, 1967, 636-638 B. B. Mandelbrot

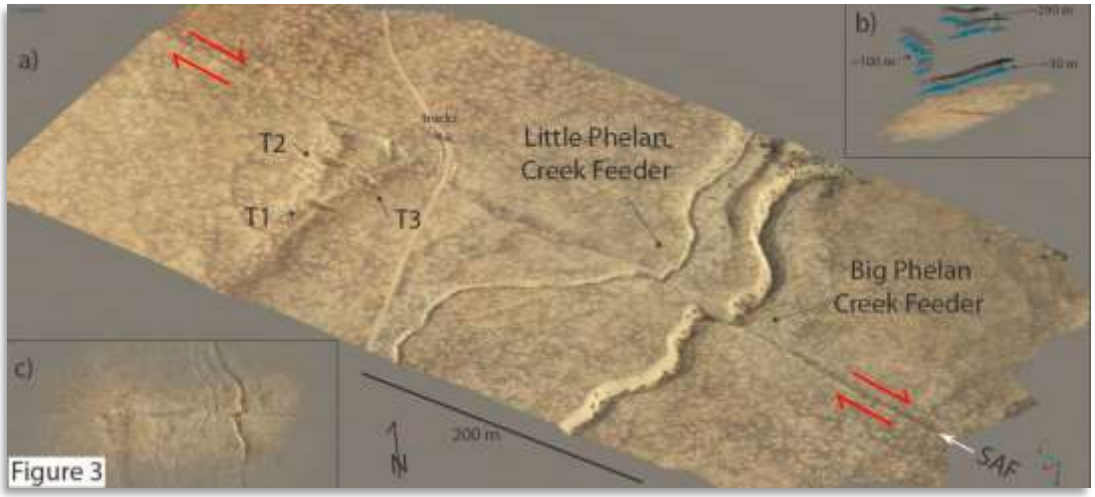

Barrett Salisbury, ASU

Shuttle Radar Topography Mission

-released in 2005

-90 m pixel size

-coverage of latitudes <60°

ASTER GDEM

-released in 2009

-30 m pixel size

-Coverage of latitudes <83°

Airborne LiDAR

-started appearing in early 2000s

-sub-meter resolution data now standard

Structure from Motion

-first used on landscapes in 2010s

-decimeter resolution achievable

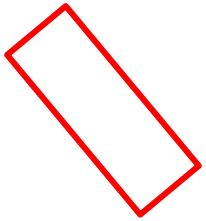

1 km

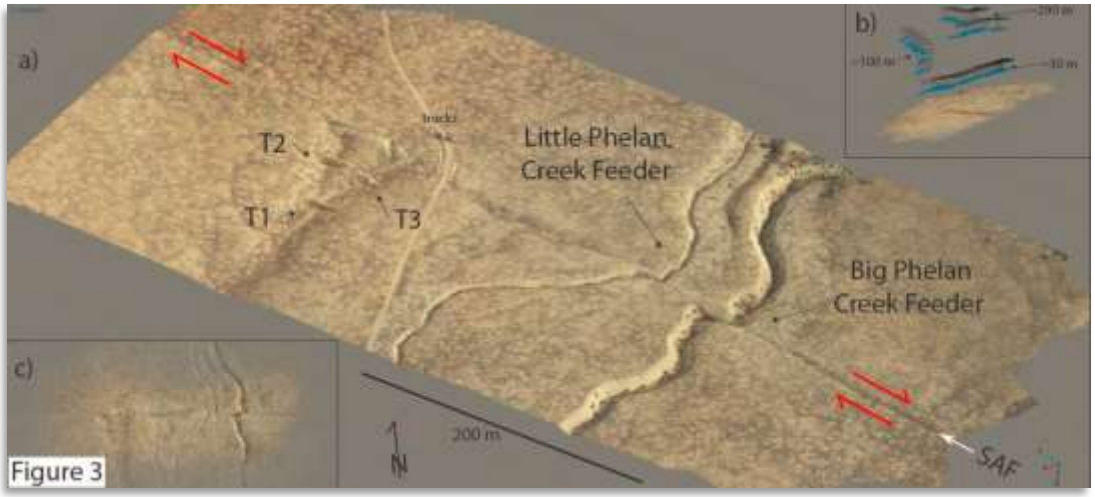

Barrett Salisbury, ASU

Shuttle Radar Topography Mission

-released in 2005

-90 m pixel size

-coverage of latitudes <60°

ASTER GDEM

-released in 2009

-30 m pixel size

-Coverage of latitudes <83°

Airborne LiDAR

-started appearing in early 2000s

-sub-meter resolution data now standard

Structure from Motion

-first used on landscapes in 2010s

-decimeter resolution achievable

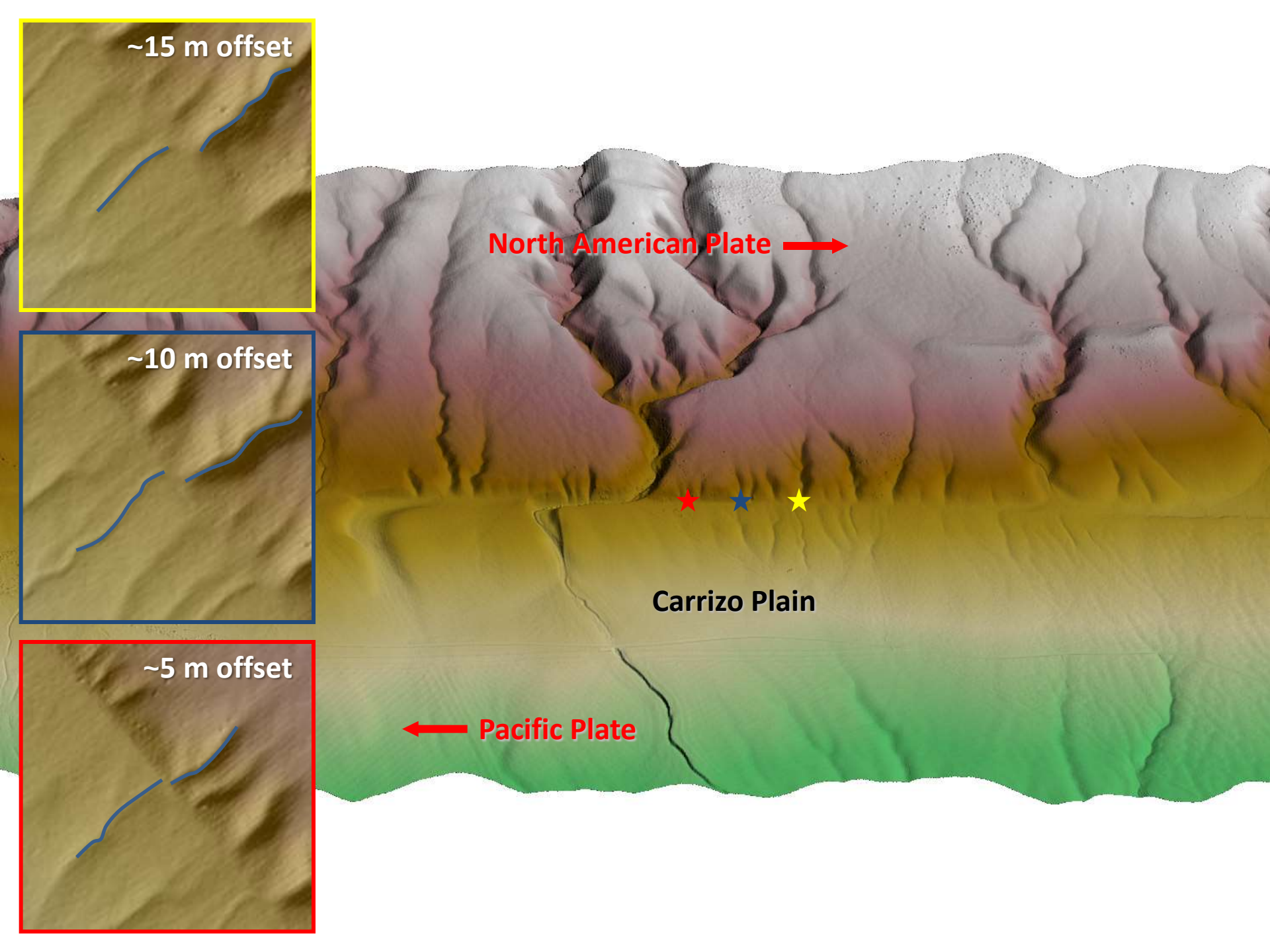
~15 m offset
~10 m offset
~5 m offset
North American Plate
Carrizo Plain
Pacific Plate

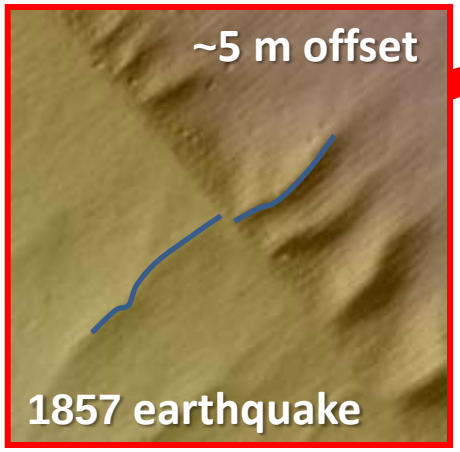

Slip in the 1857 and Earlier Large Earthquakes Along the Carrizo Plain, San Andreas Fault

Olaf Zielke,[1*] J Ramón Arrowsmith,[1] Lisa Grant Ludwig,[2] Sinan O. Akçiz[2]

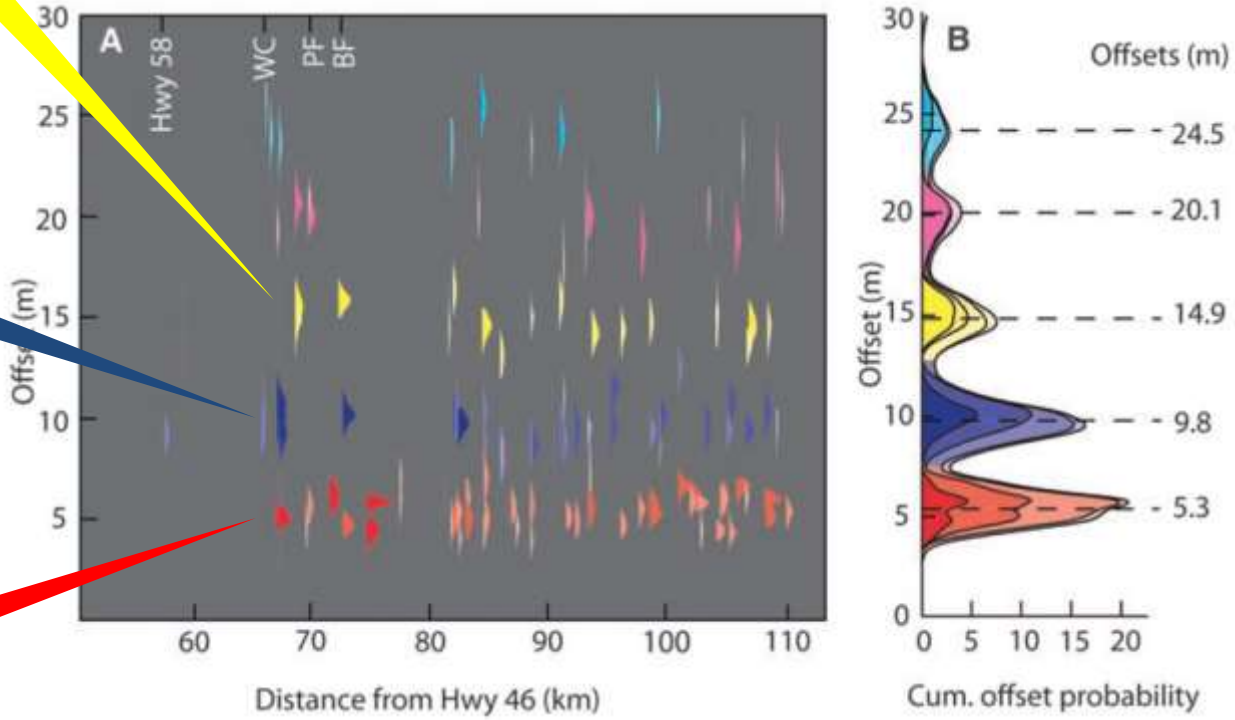

Single high-resolution topography datasets

=> potential for long-term earthquake histories

3-D earthquake displacements from repeat LiDAR

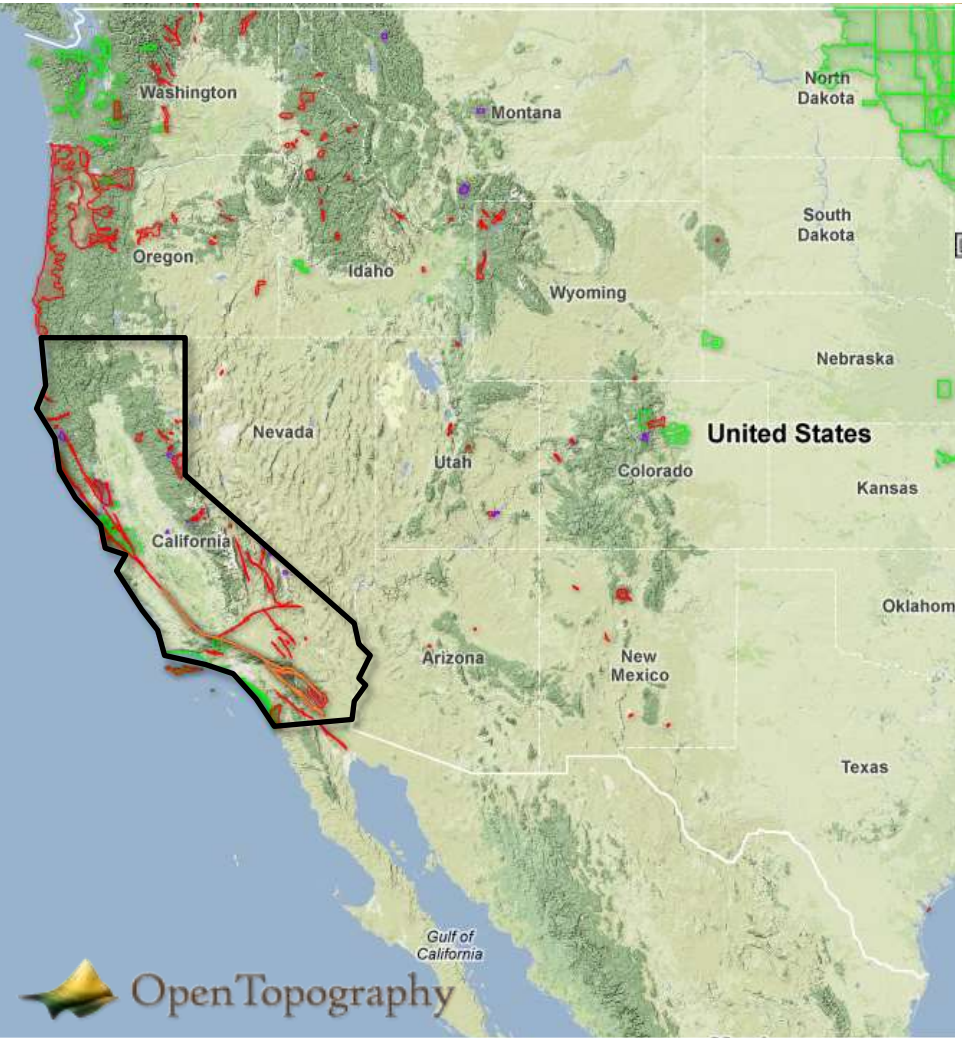

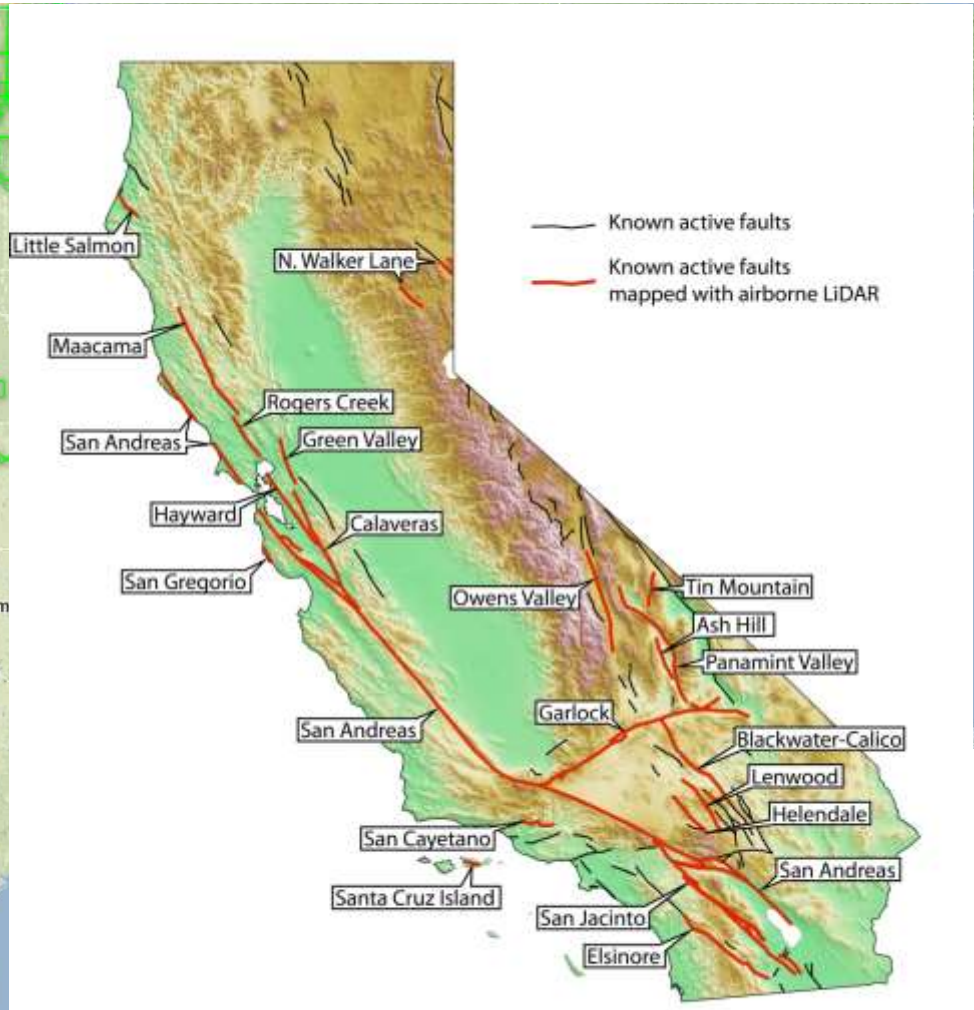

- "Baseline" of LiDAR topography now available on many active faults
- After an earthquake, repeat LiDAR data can be collected and 3-D displacements imaged

3-D earthquake displacements from repeat LiDAR

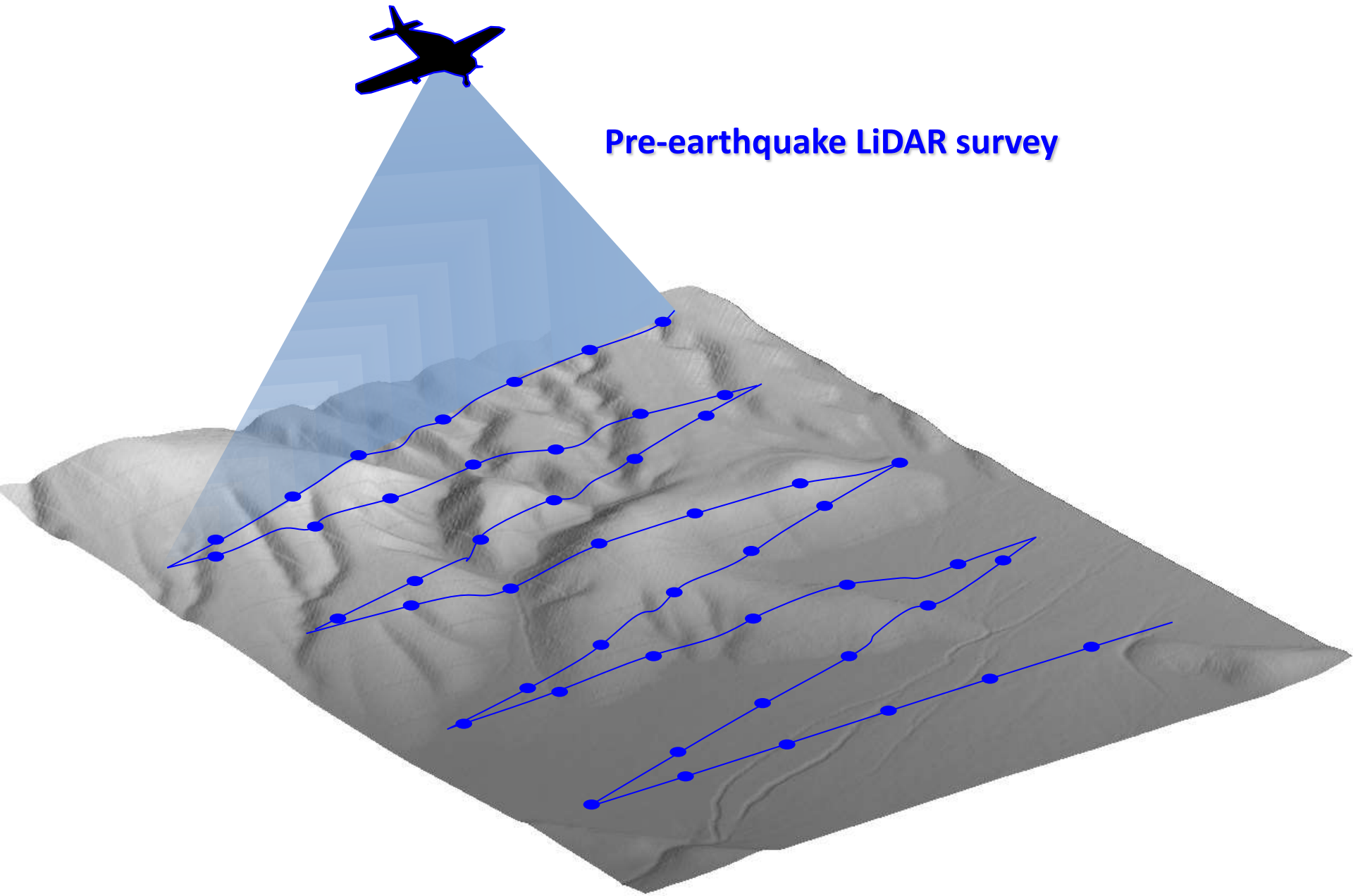

3-D earthquake displacements from repeat LiDAR

Pre-earthquake point cloud

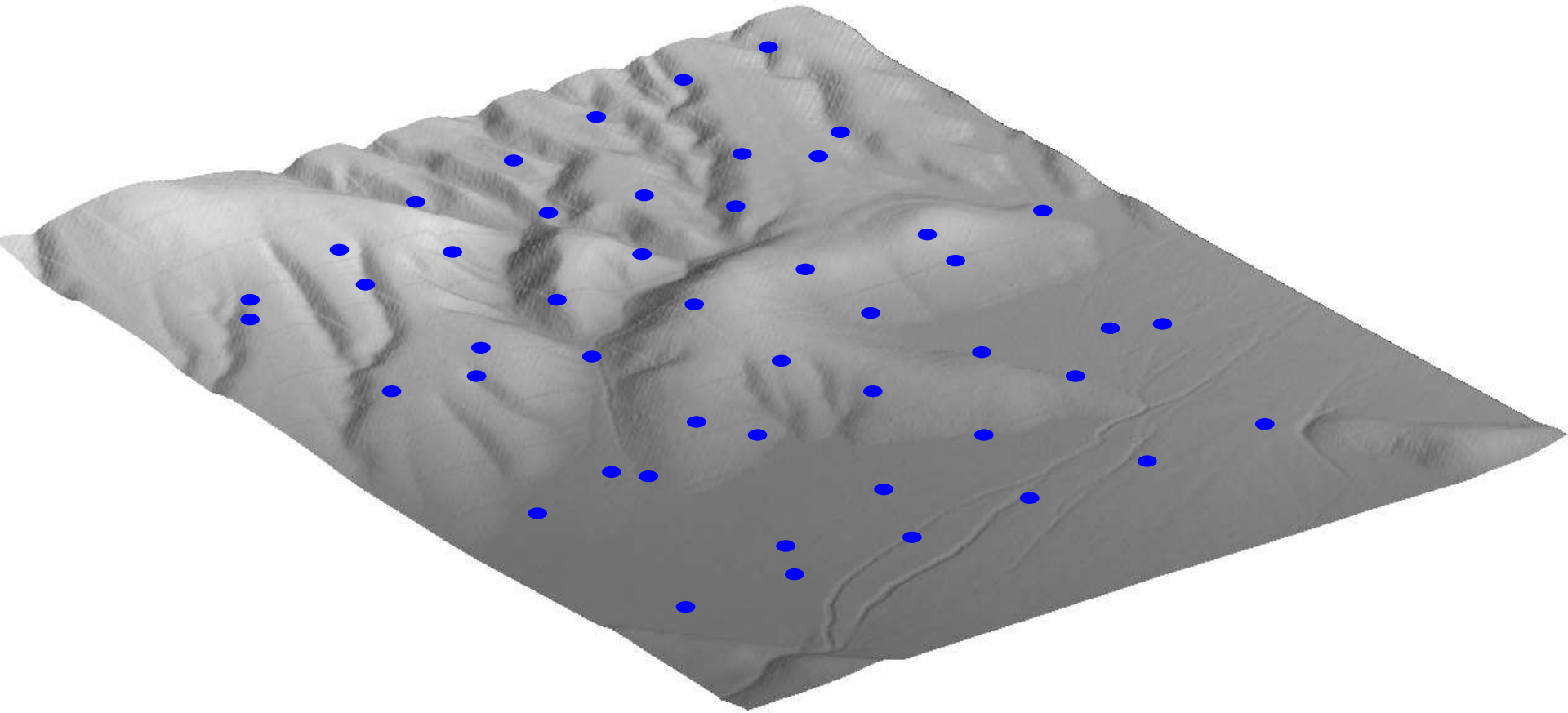

3-D earthquake displacements from repeat LiDAR

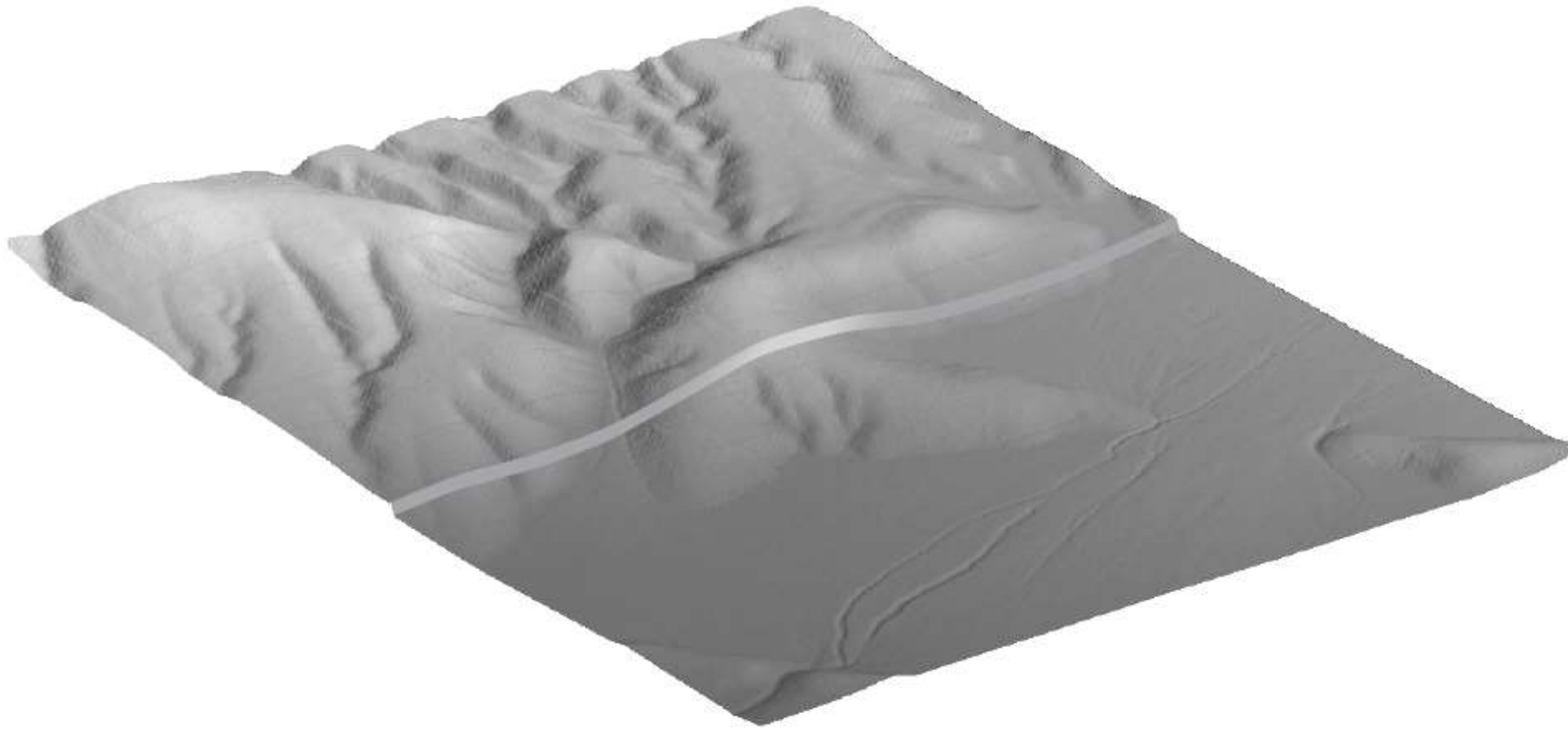

3-D earthquake displacements from repeat LiDAR

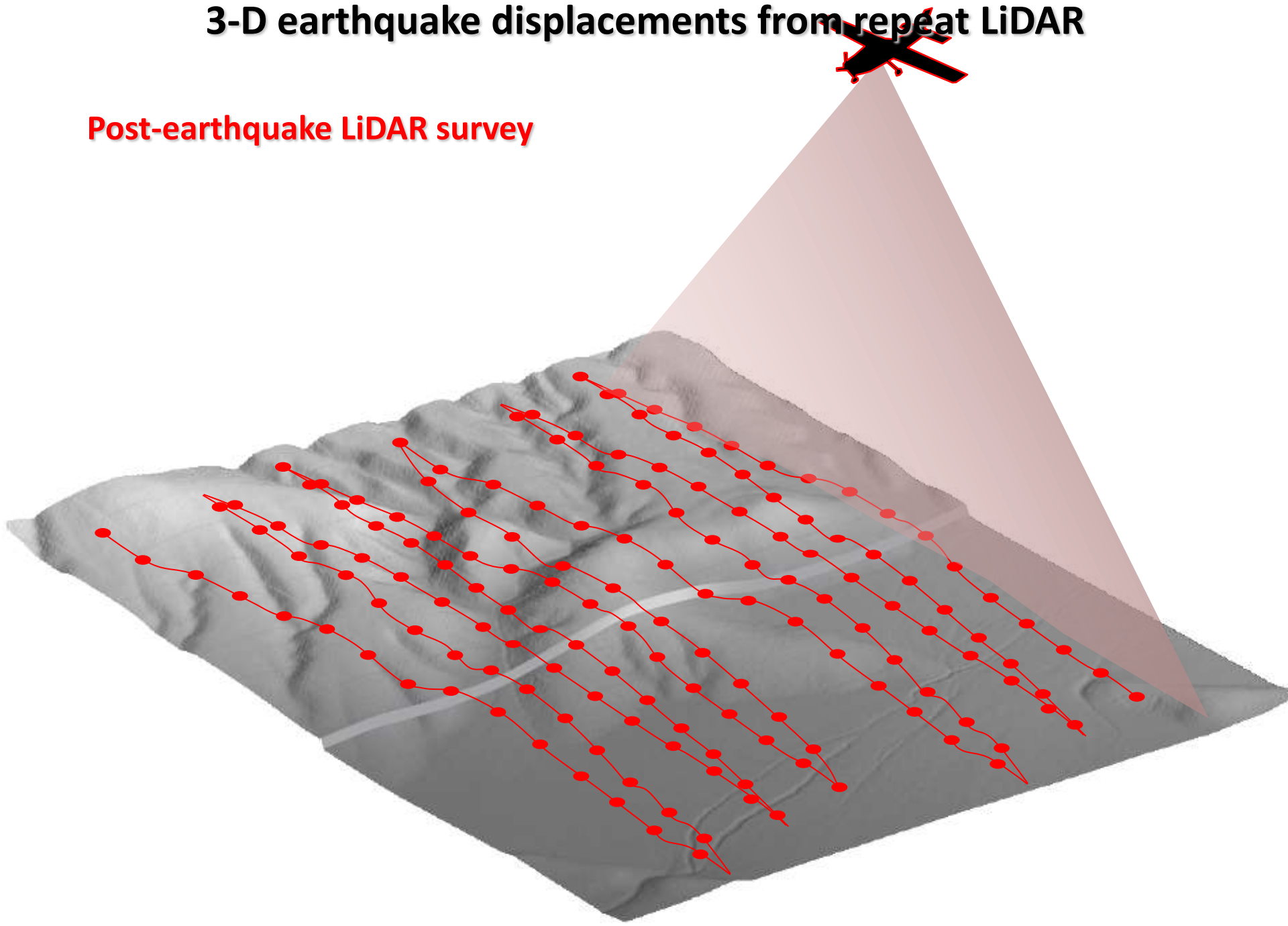

3-D earthquake displacements from repeat LiDAR

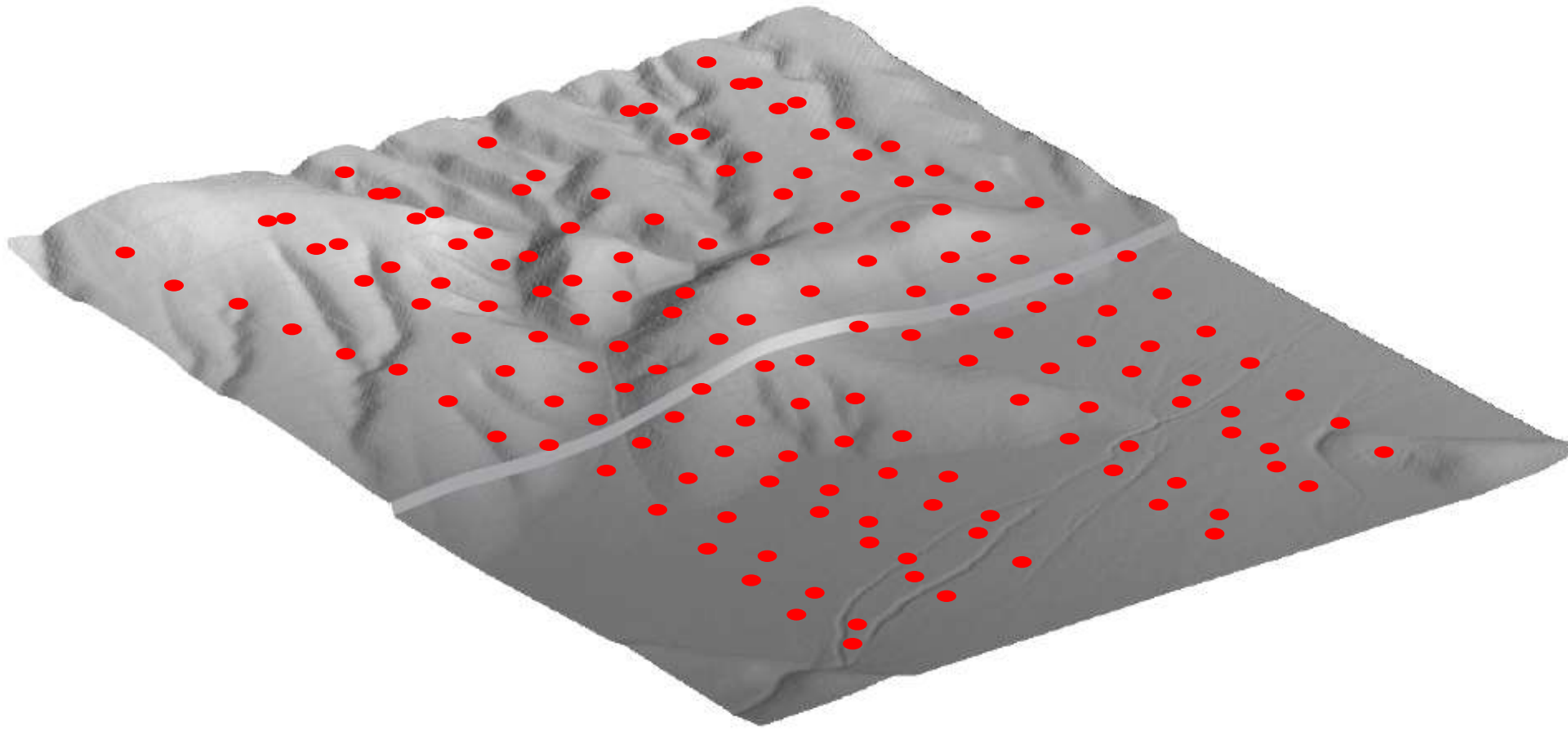

3-D earthquake displacements from repeat LiDAR

Pre-earthquake point cloud

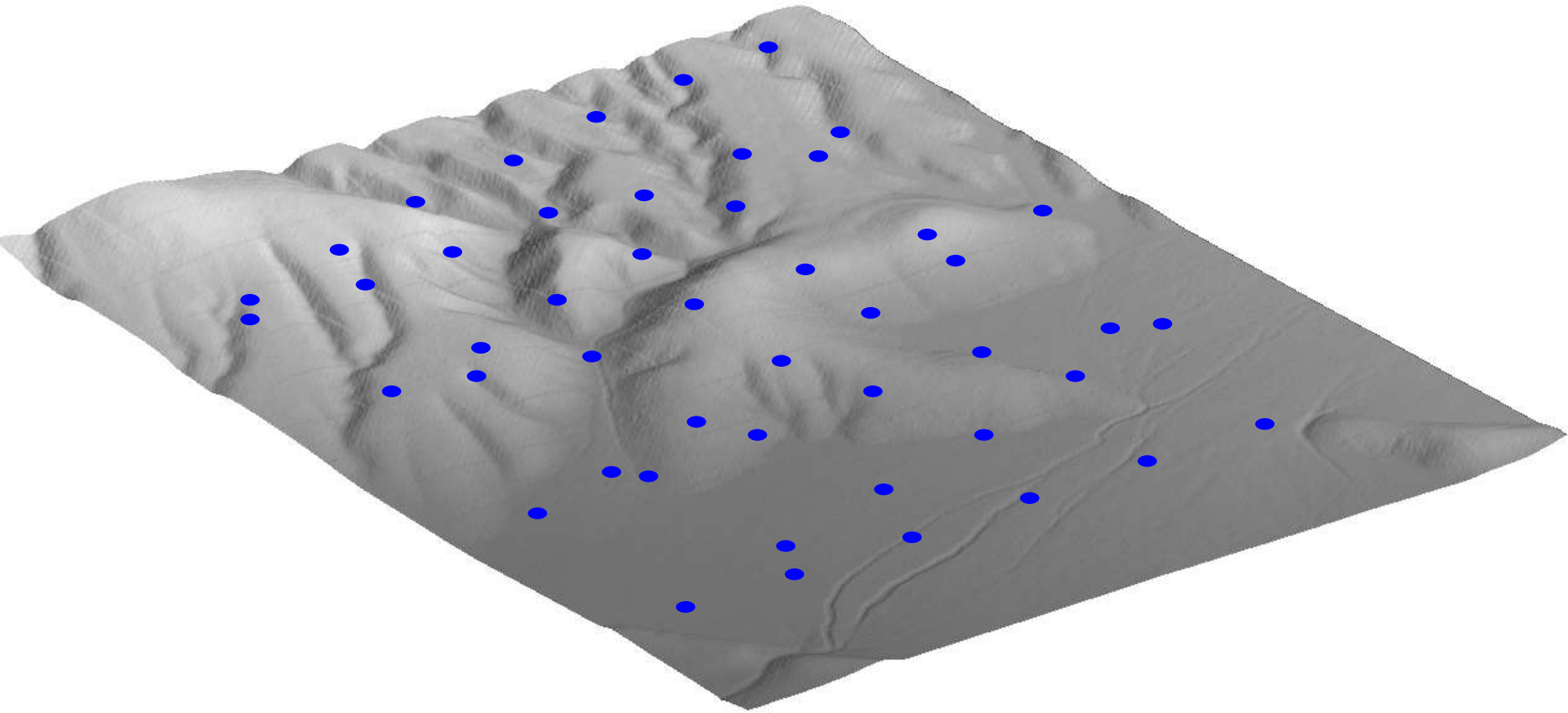

3-D earthquake displacements from repeat LiDAR

Pre-earthquake point cloud

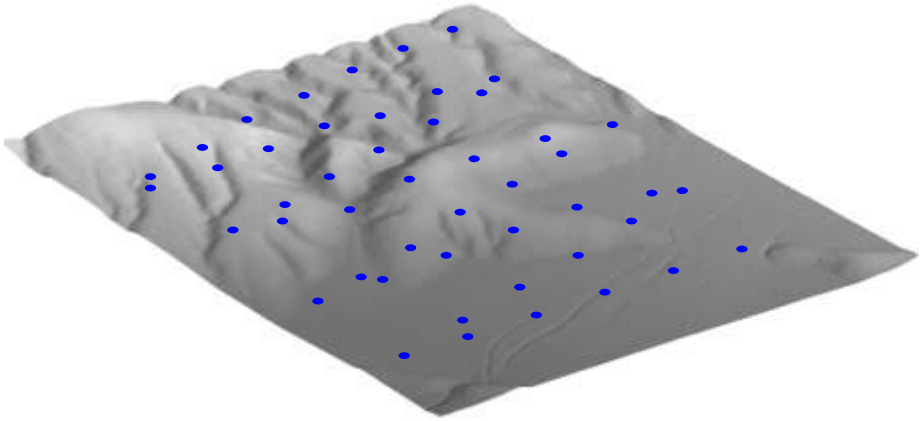

Post-earthquake point cloud

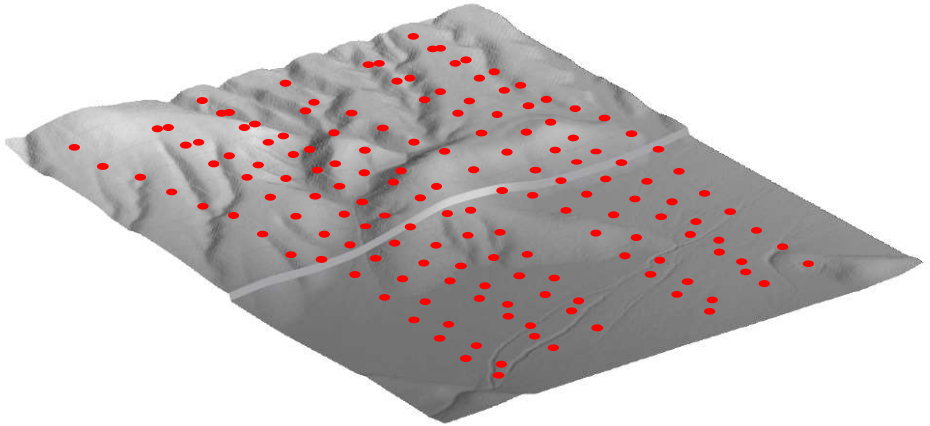

The Challenges of LiDAR differencing

- Data are irregularly spaced (we can rasterize them, but lose information doing so)

- There can be large mismatches in point density (typically the newer dataset is denser)

- The **Iterative Closest Point (ICP)** algorithm overcomes these problems

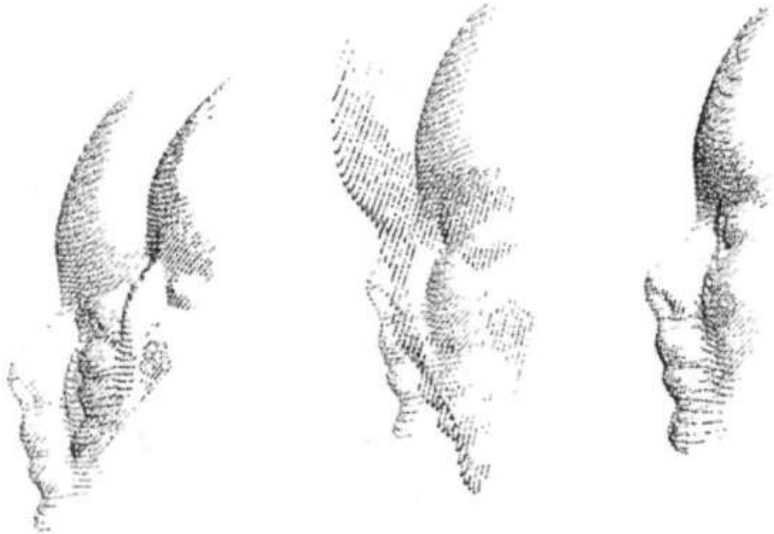

Fig. 4. Iterative point-based registration of phantom face range data

3-D earthquake displacements from repeat LiDAR

Pre-earthquake point cloud

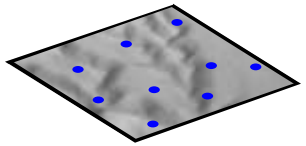

Post-earthquake point cloud

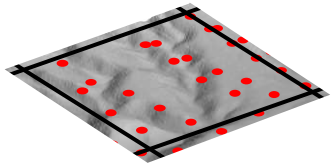

- the two point clouds are first split into square “windows”, 50 m in diameter
- ICP is run separately on each pair of windows, finding the rigid-body **translation** and **rotation** that best aligns them
- this alignment corresponds to the local earthquake displacement for that window.

GEOPHYSICAL RESEARCH LETTERS, VOL. 39, L16301, doi:10.1029/2012GL052460, 2012

Three-dimensional surface displacements and rotations from differencing pre- and post-earthquake LiDAR point clouds

Edwin Nissen,[1,2] Aravindhan K. Krishnan,[1] J. Ramón Arrowsmith,[1] and Srikanth Saripalli[1]

3-D earthquake displacements from repeat LiDAR

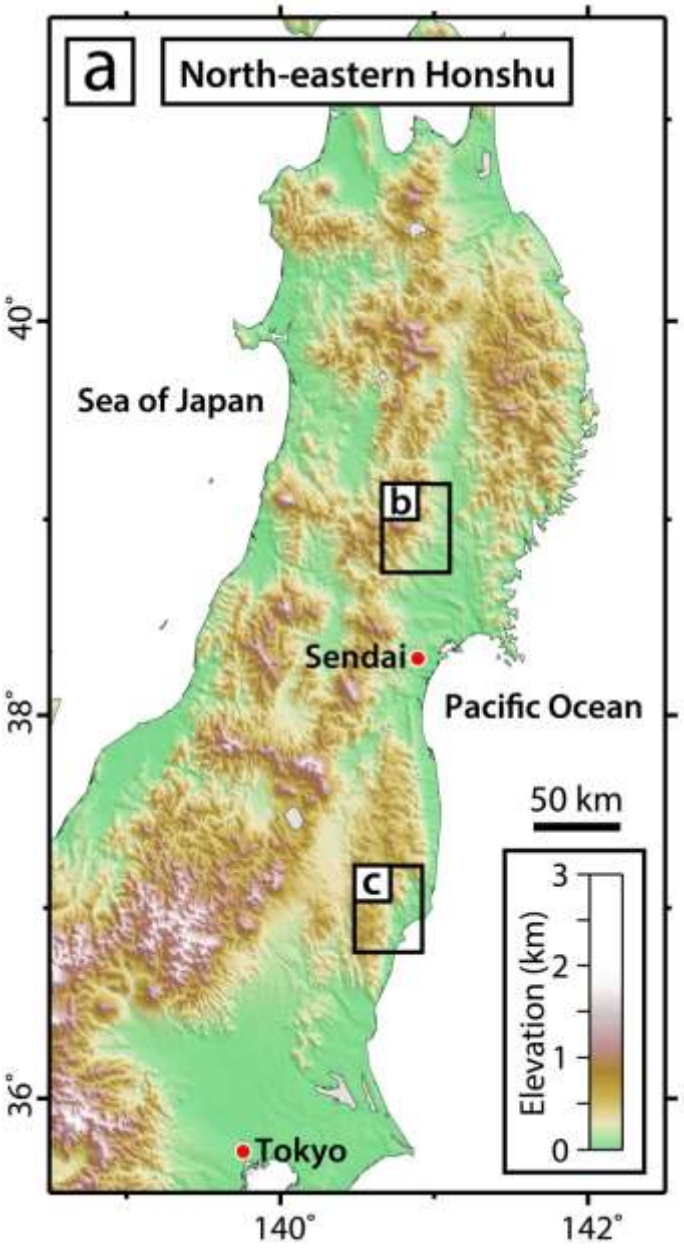

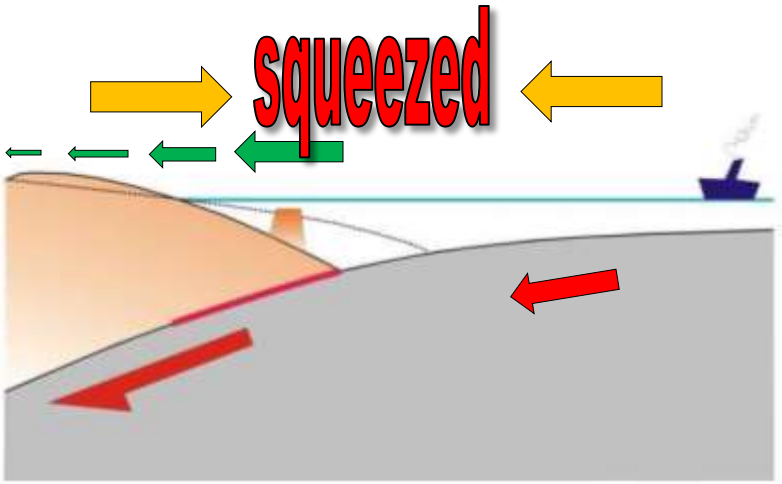

between earthquakes elastic strain accumulates

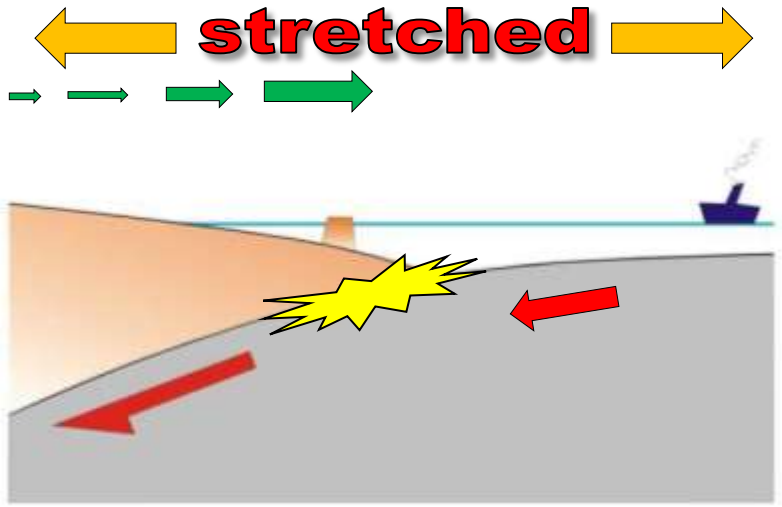

during earthquake elastic strain is released

3-D earthquake displacements from repeat LiDAR

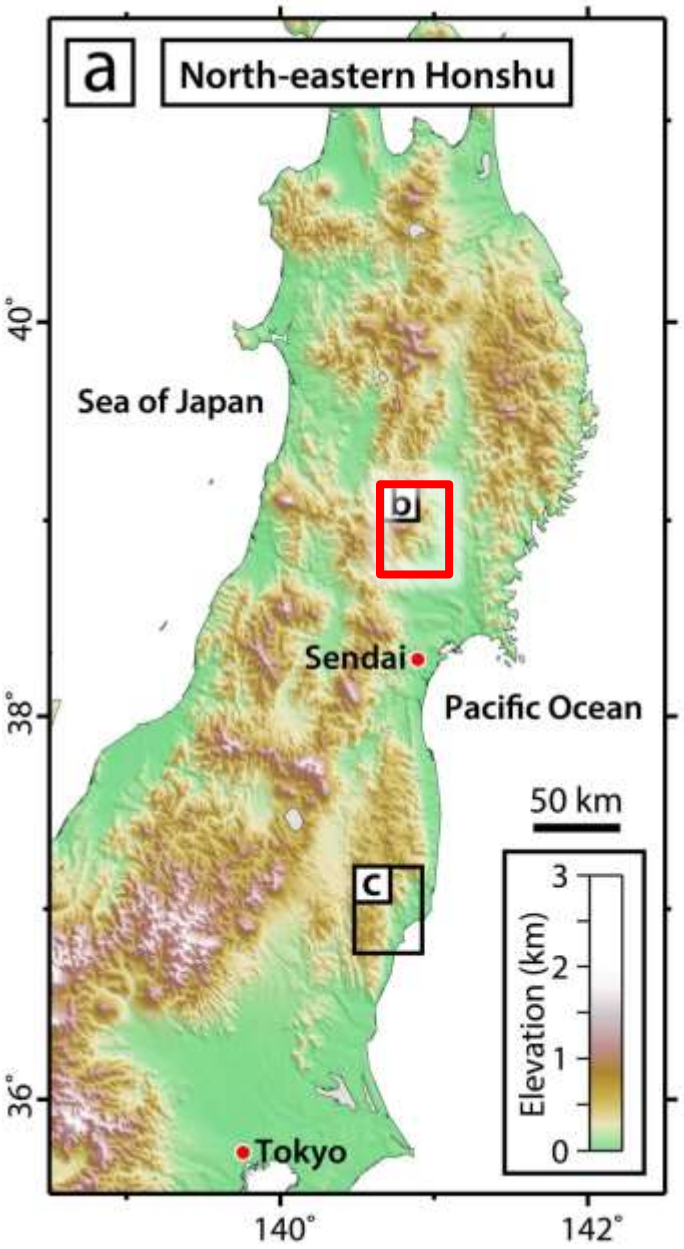

3-D earthquake displacements from repeat LiDAR

The 2008 Iwate-Miyagi earthquake (Mw 6.9), Japan

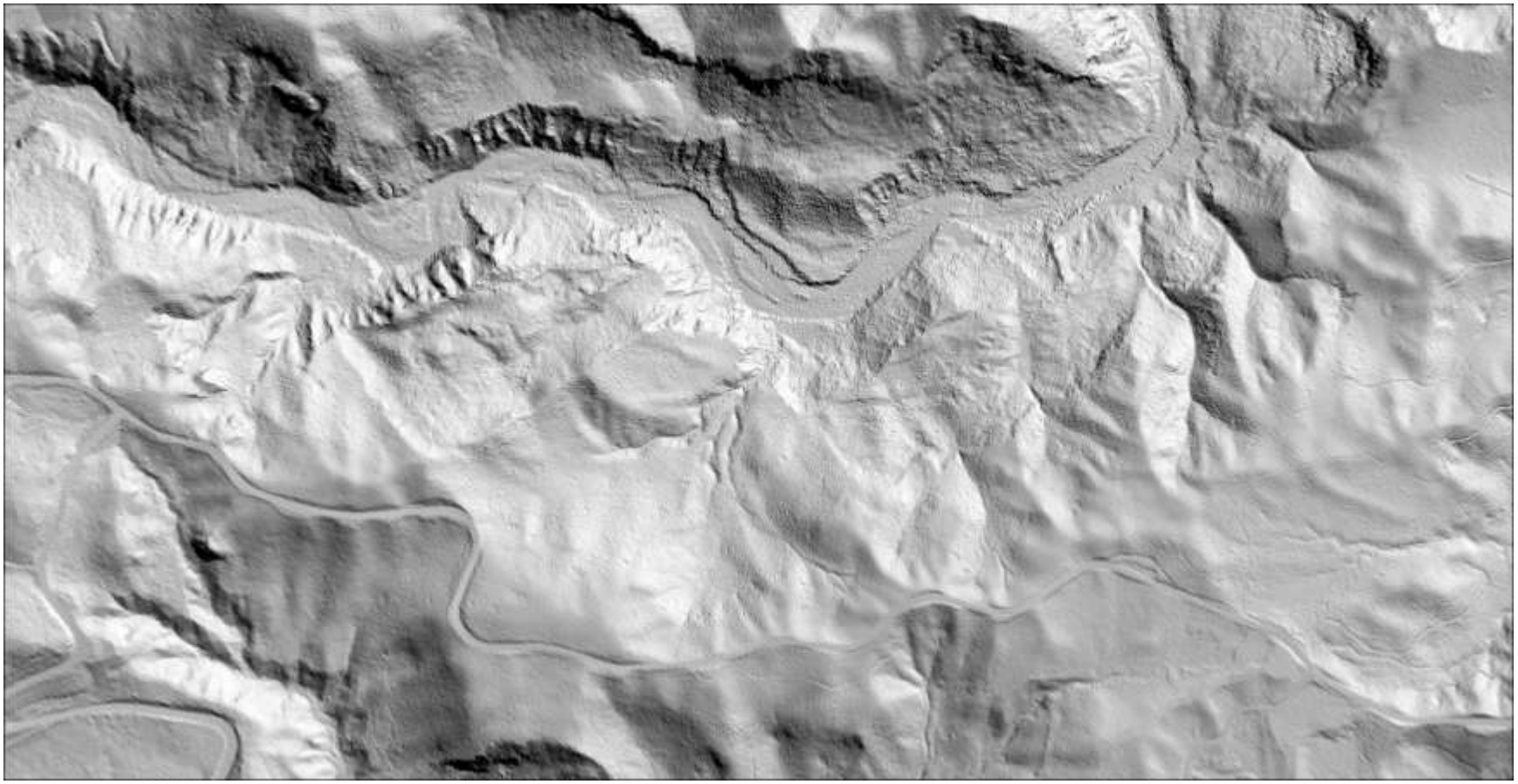

Pre-earthquake DEM (2m)

KOKUSAI KOGYO GROUP

3-D earthquake displacements from repeat LiDAR

The 2008 Iwate-Miyagi earthquake (Mw 6.9), Japan

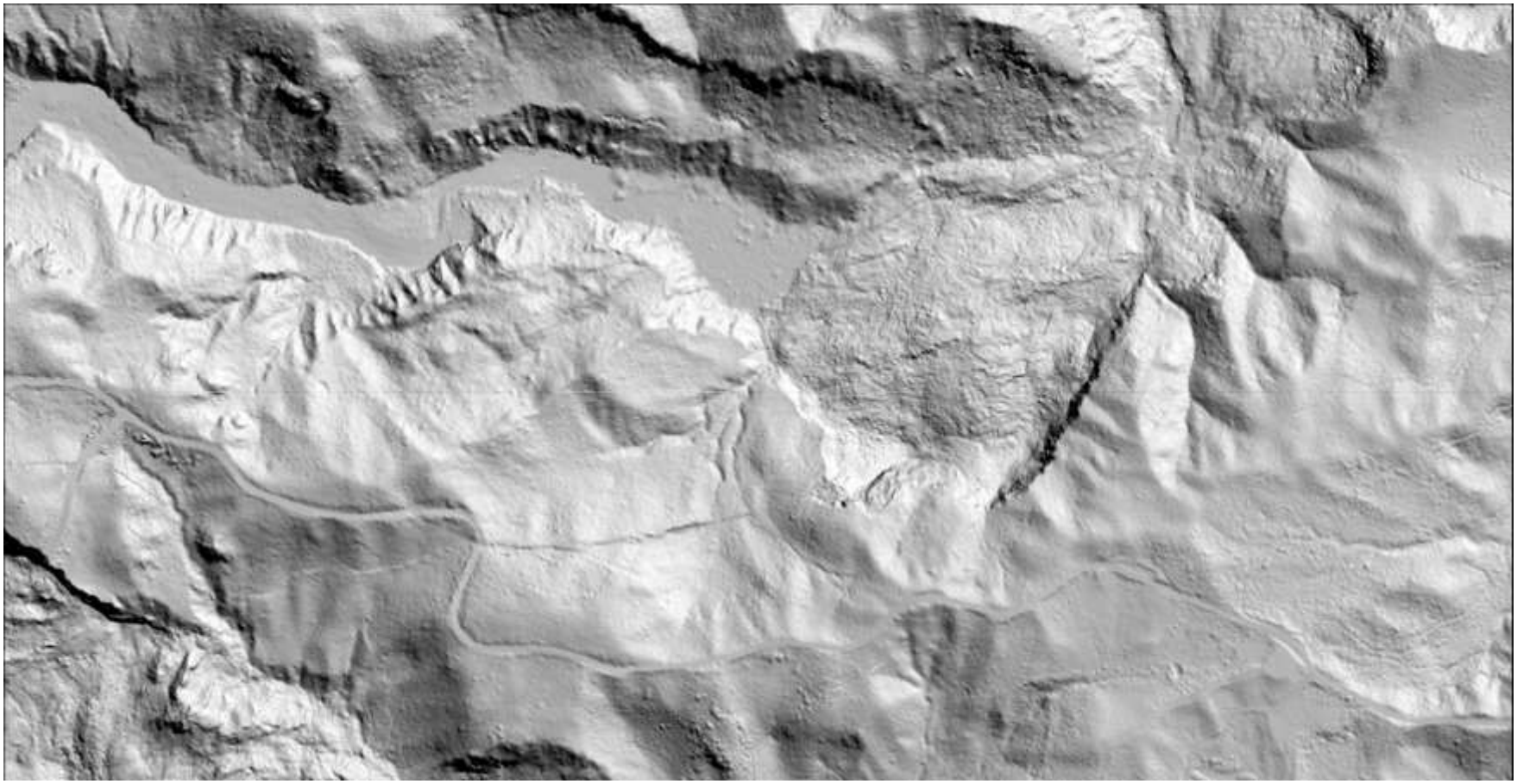

Post-earthquake DEM (1m)

AERO ASAHI CORPORATION

3-D earthquake displacements from repeat LiDAR

The 2008 Iwate-Miyagi earthquake (Mw 6.9), Japan

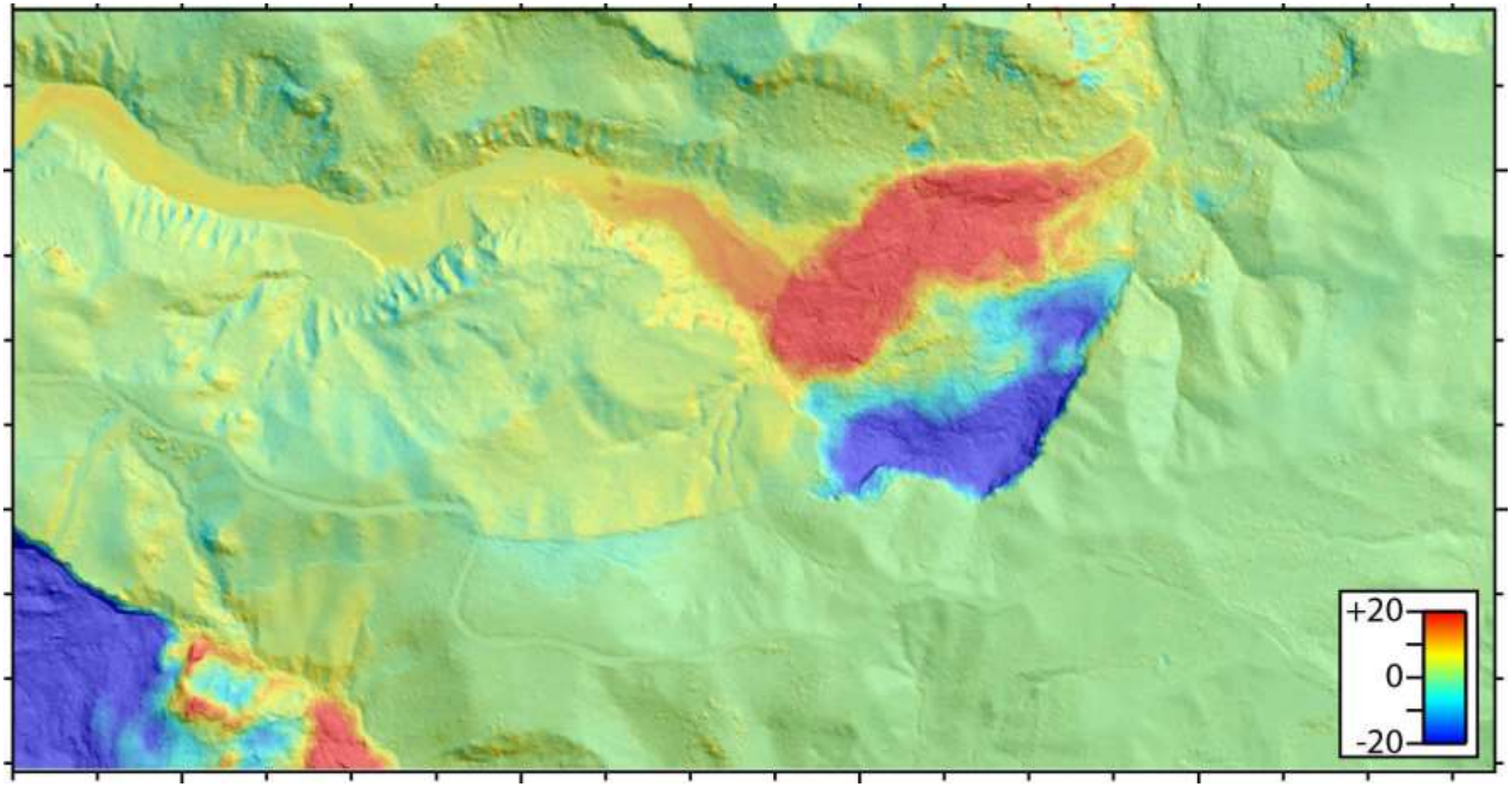

DEM subtraction (height change, m)

3-D earthquake displacements from repeat LiDAR

The 2008 Iwate-Miyagi earthquake (Mw 6.9), Japan

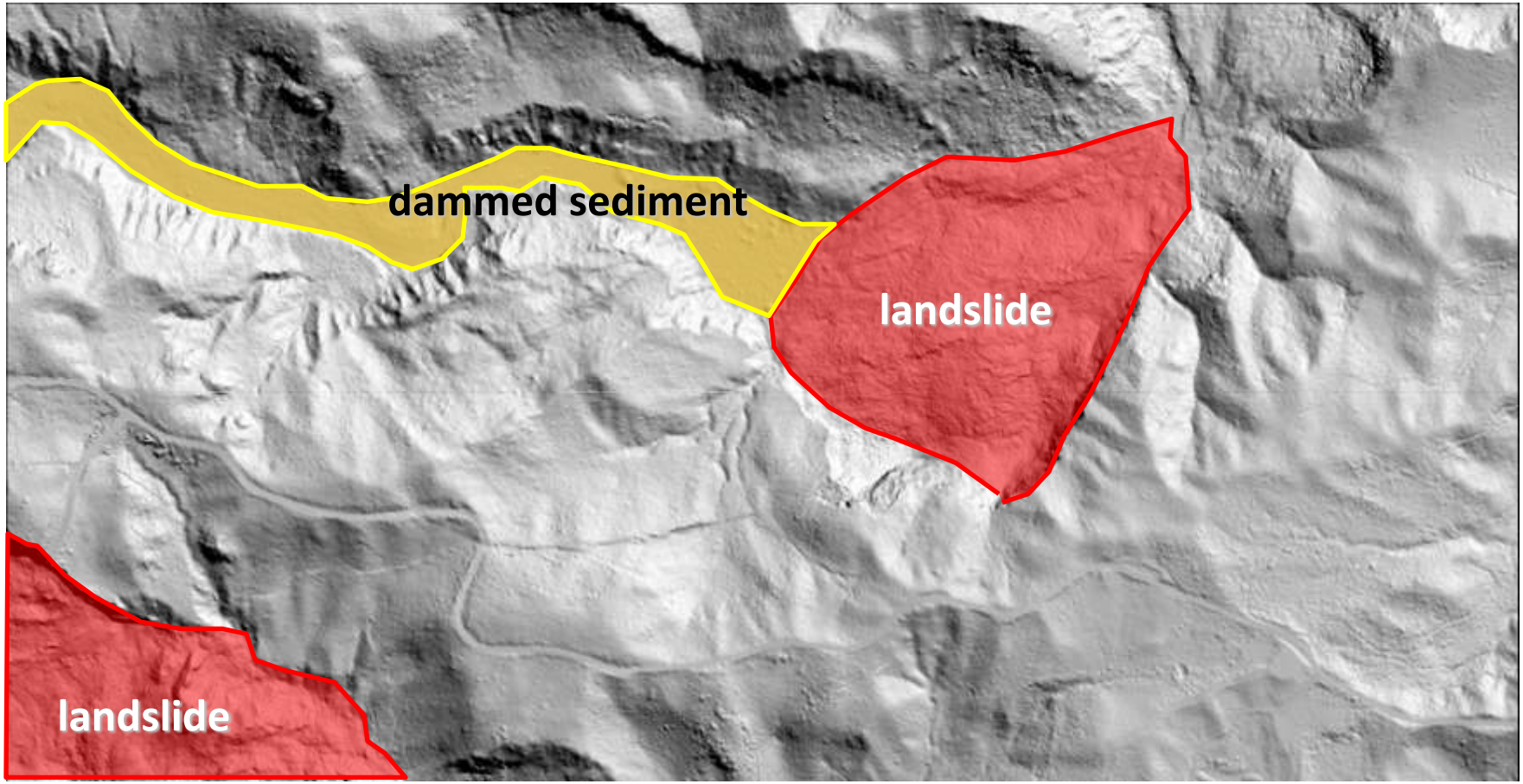

3-D earthquake displacements from repeat LiDAR

The 2008 Iwate-Miyagi earthquake (Mw 6.9), Japan

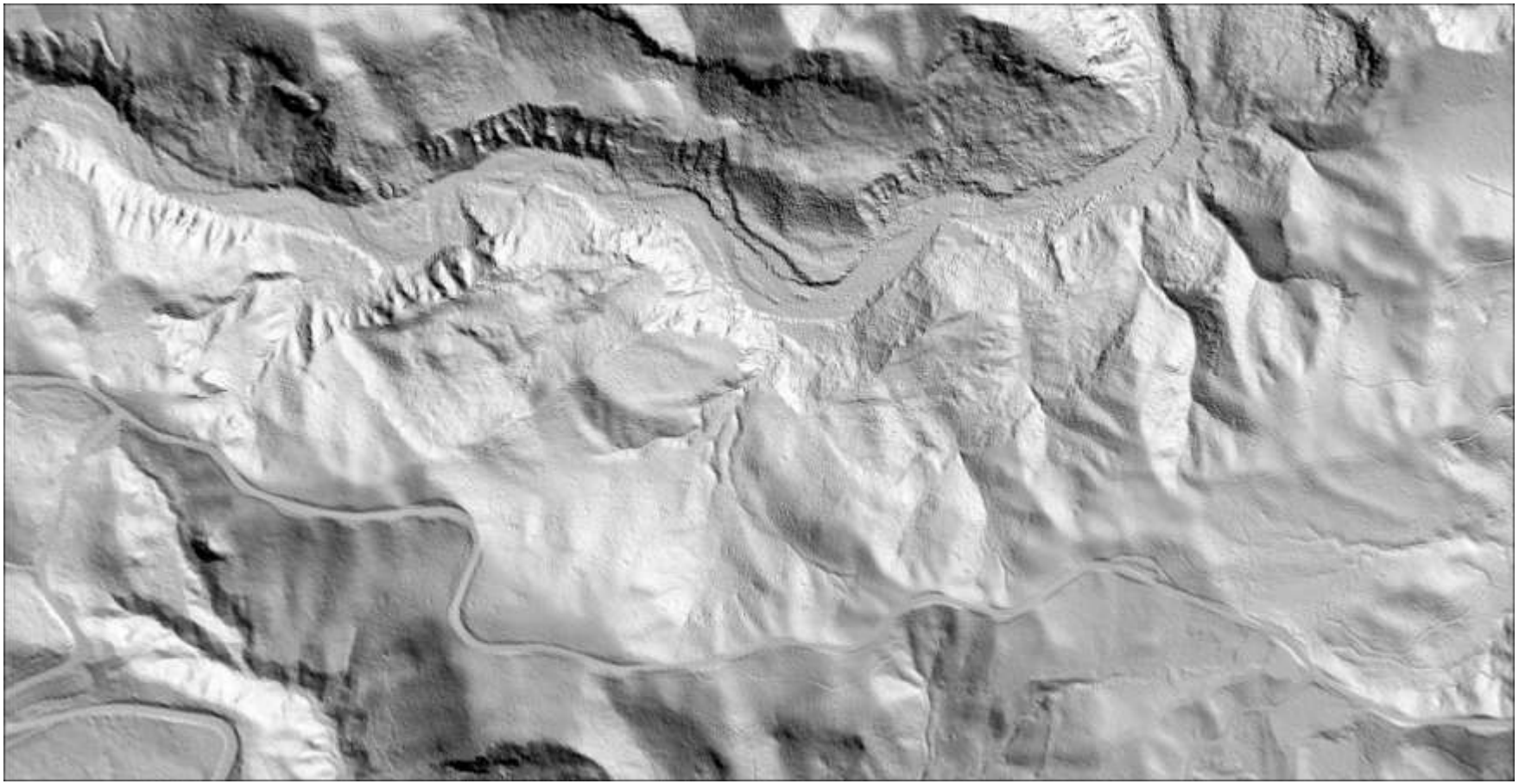

Pre-earthquake DEM (2m)

3-D earthquake displacements from repeat LiDAR

The 2008 Iwate-Miyagi earthquake (Mw 6.9), Japan

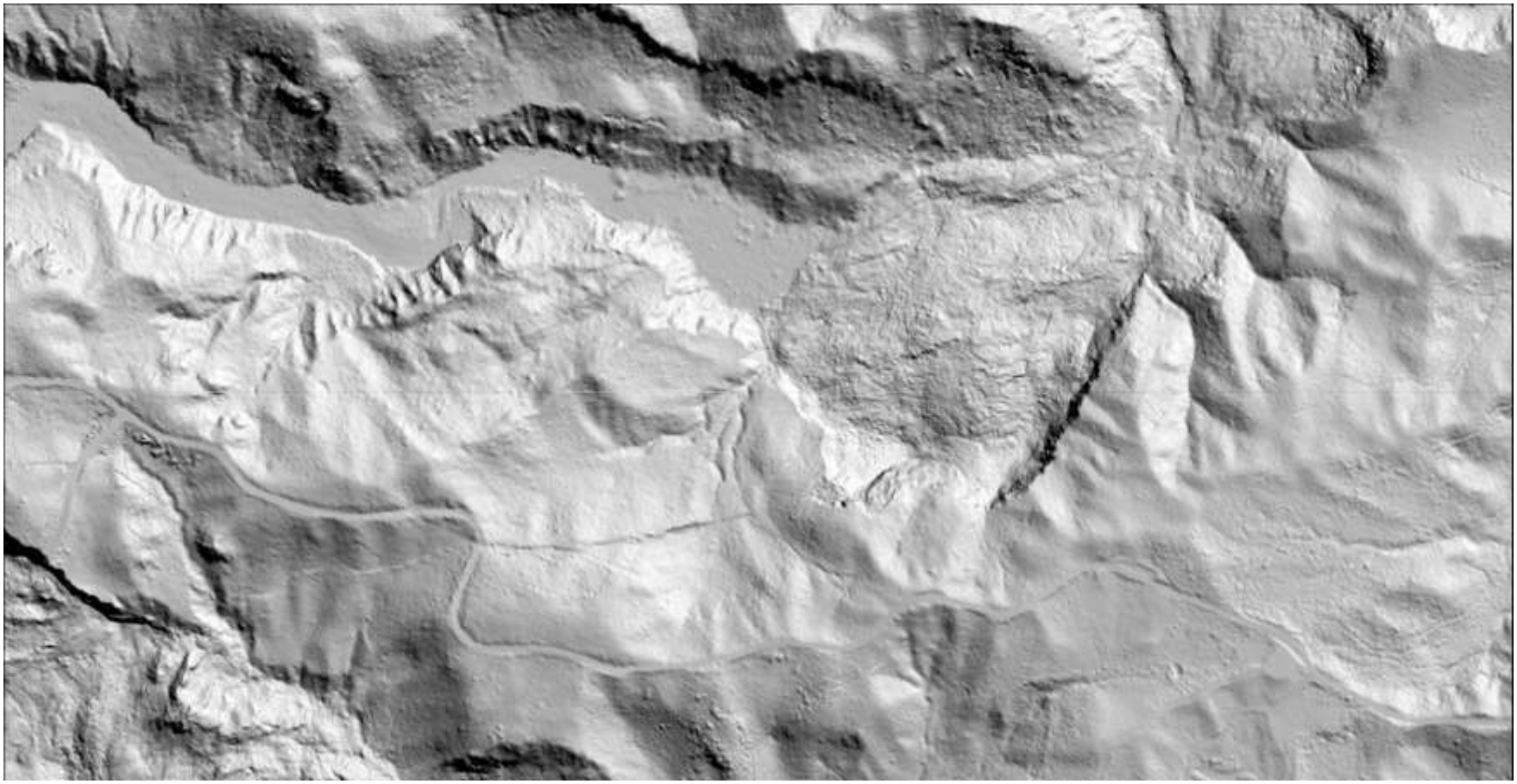

Post-earthquake DEM (1m)

3-D earthquake displacements from repeat LiDAR

The 2008 Iwate-Miyagi earthquake (Mw 6.9), Japan

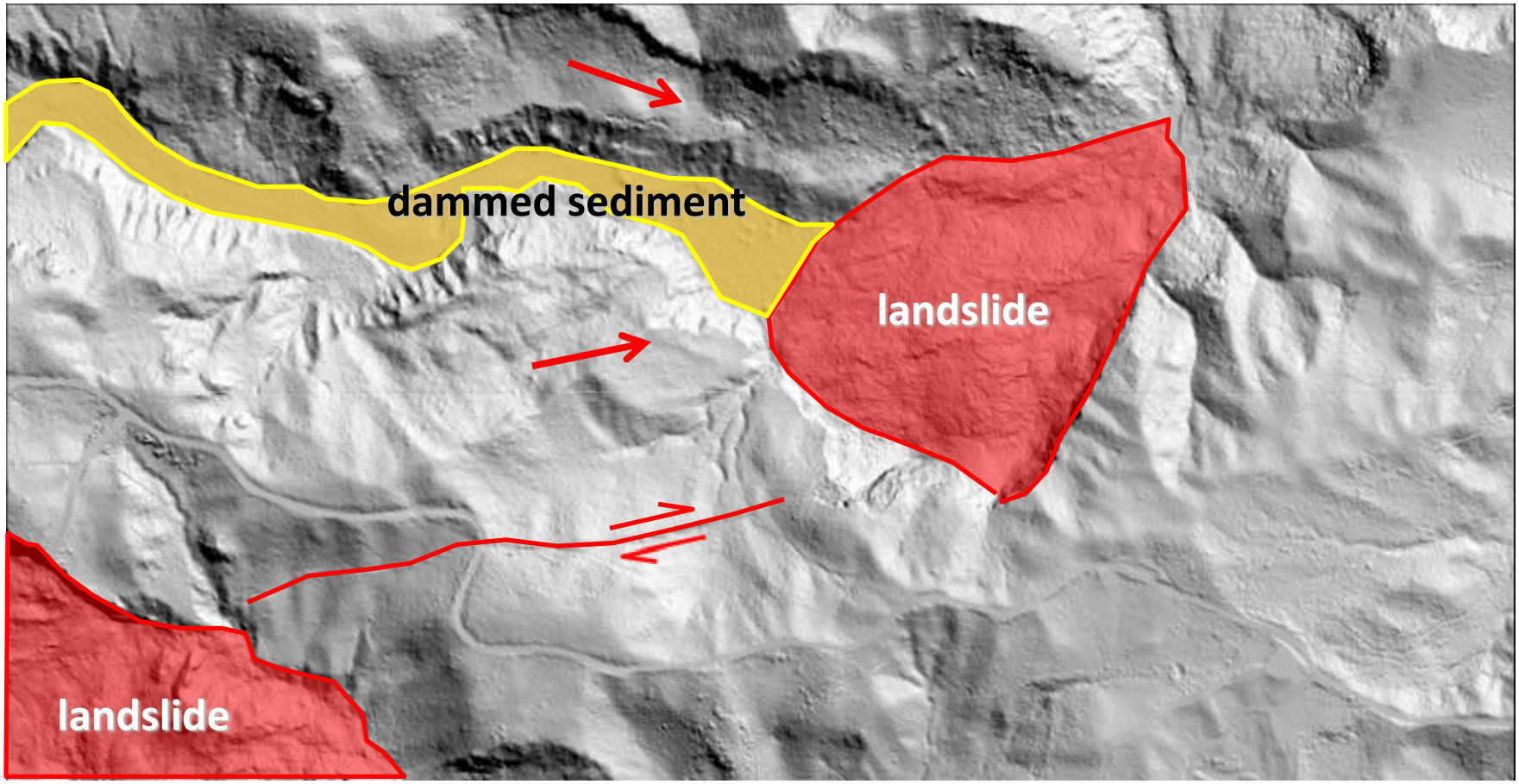

3-D earthquake displacements from repeat LiDAR

The 2008 Iwate-Miyagi earthquake (Mw 6.9), Japan

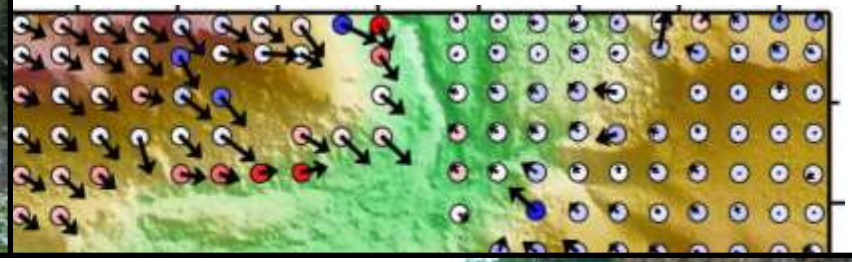

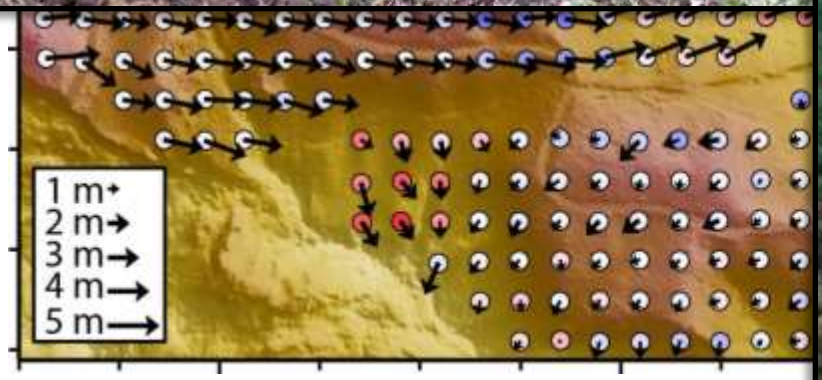

Photos by Tadashi Maruyama

3-D earthquake displacements from repeat LiDAR

The 2011 Iwaki earthquake (Mw 6.7), Japan

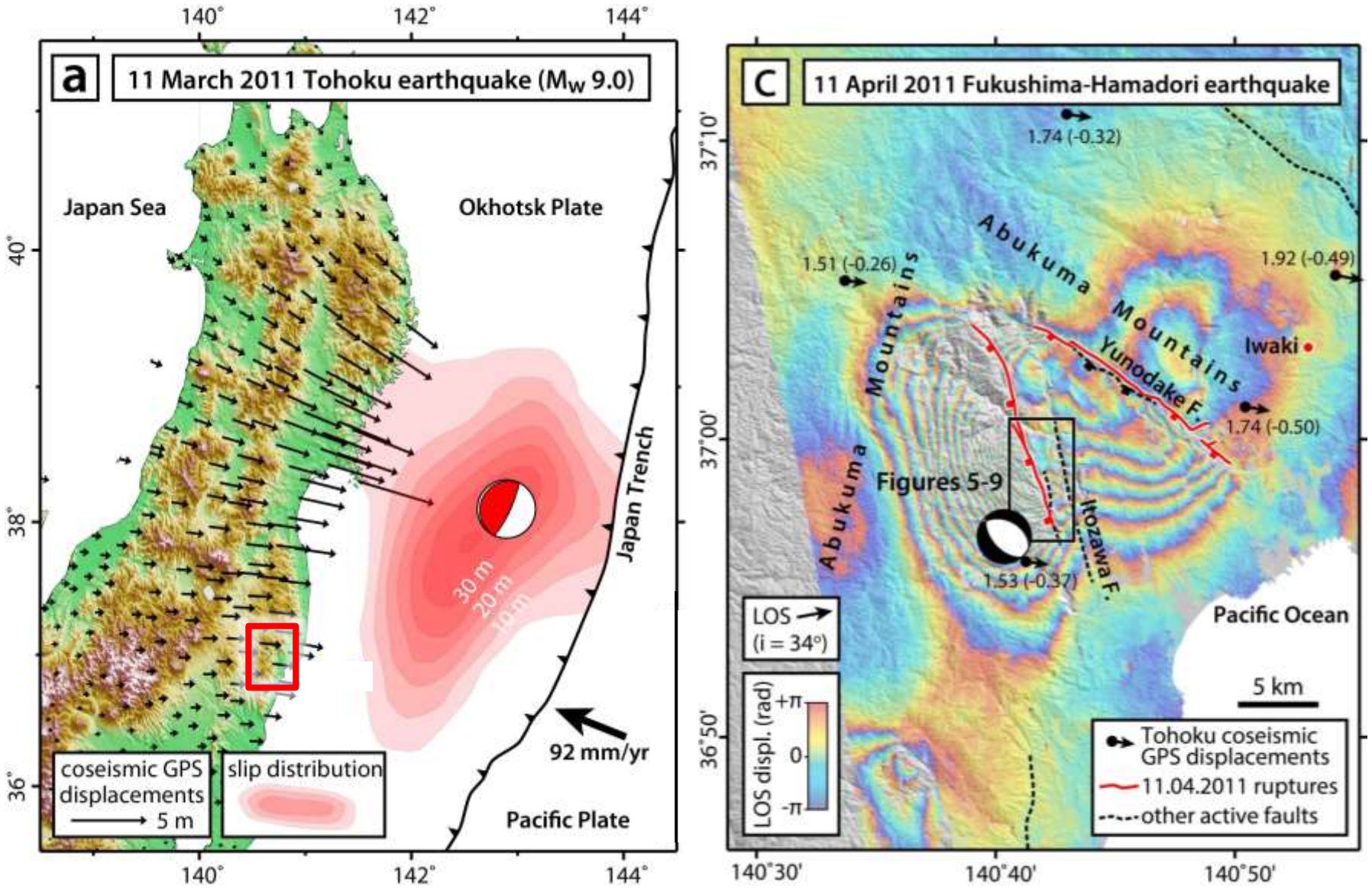

3-D earthquake displacements from repeat LiDAR

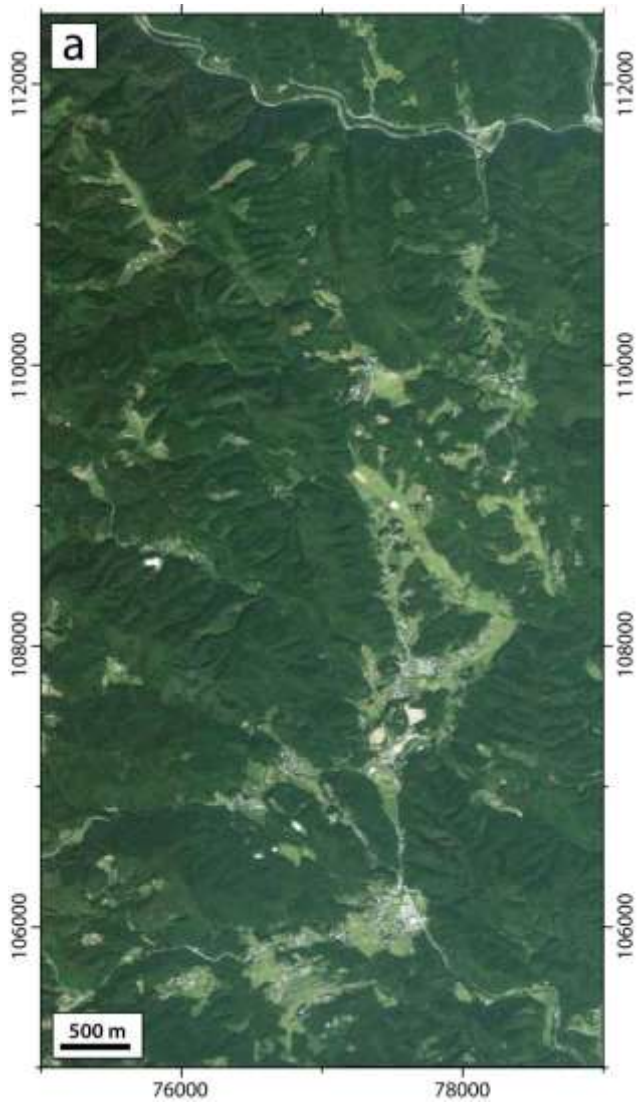

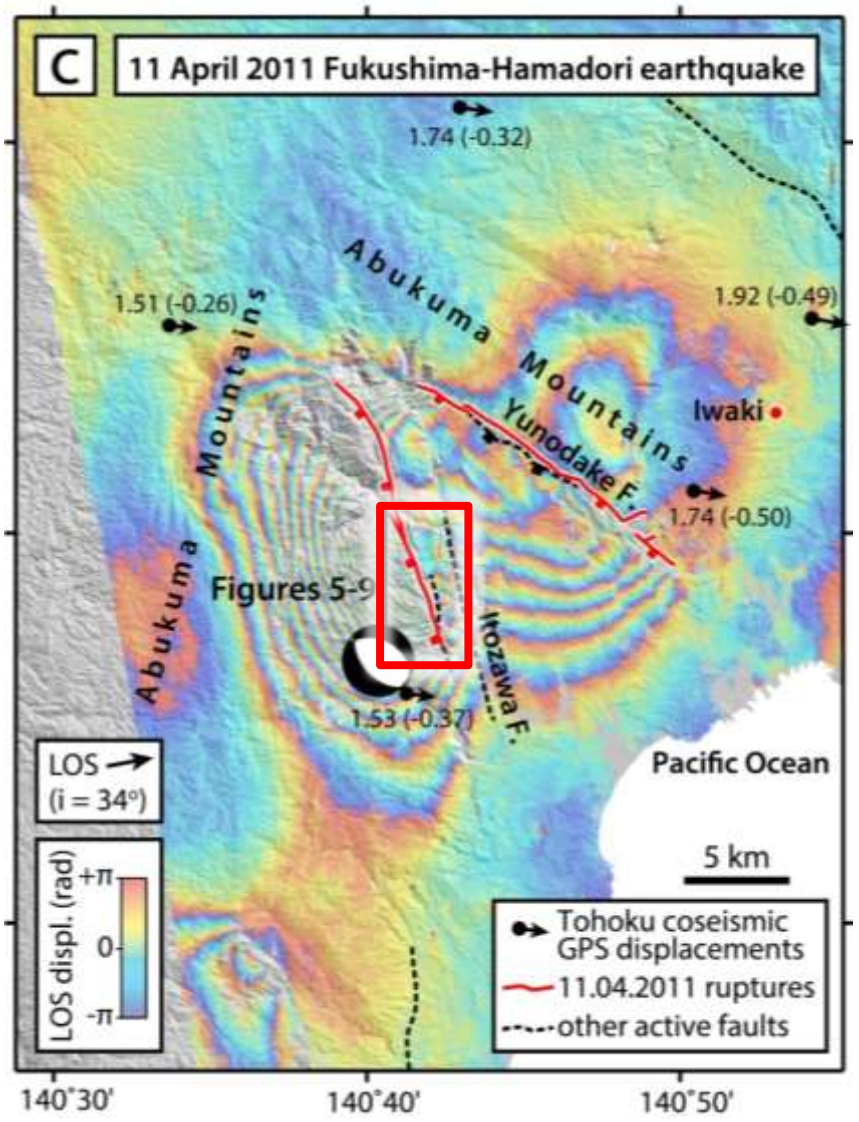

3-D earthquake displacements from repeat LiDAR

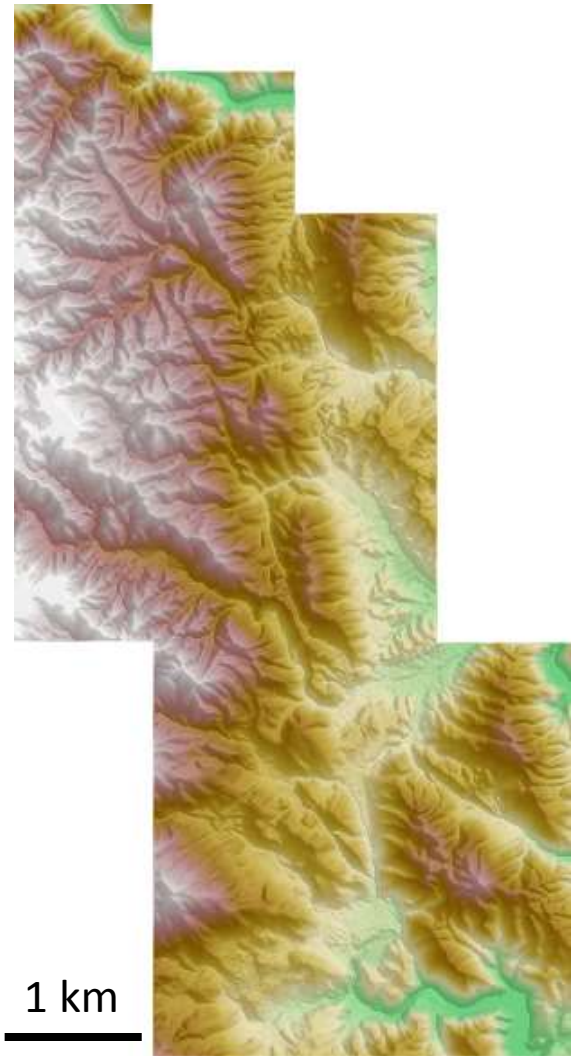

Pre-event 2 m DEM

KOKUSAI KOGYO GROUP

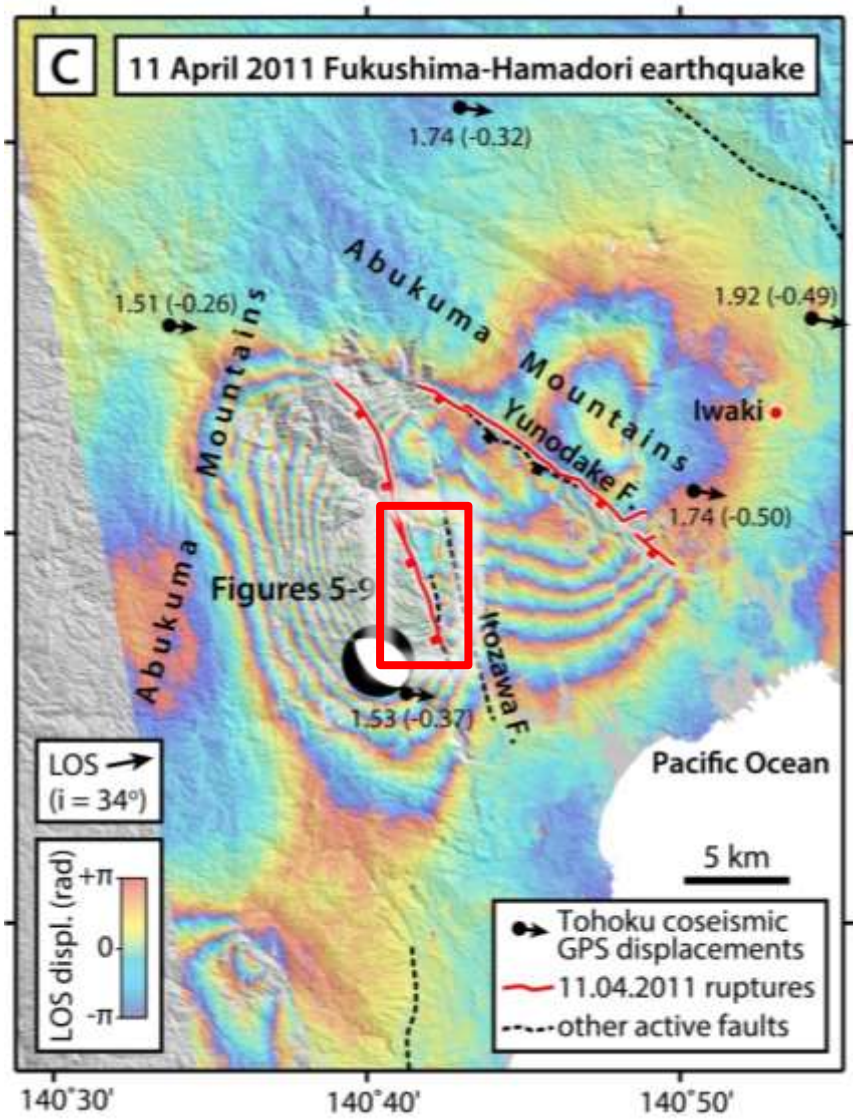

3-D earthquake displacements from repeat LiDAR

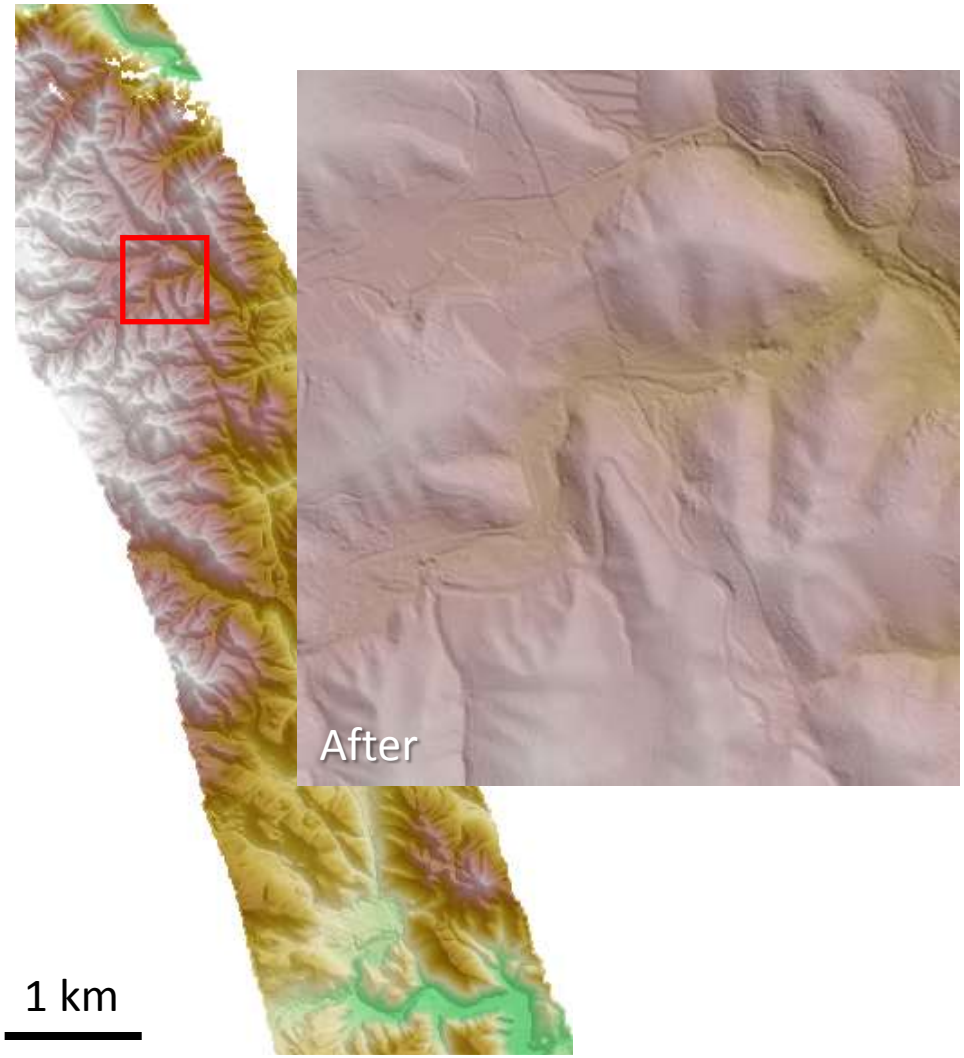

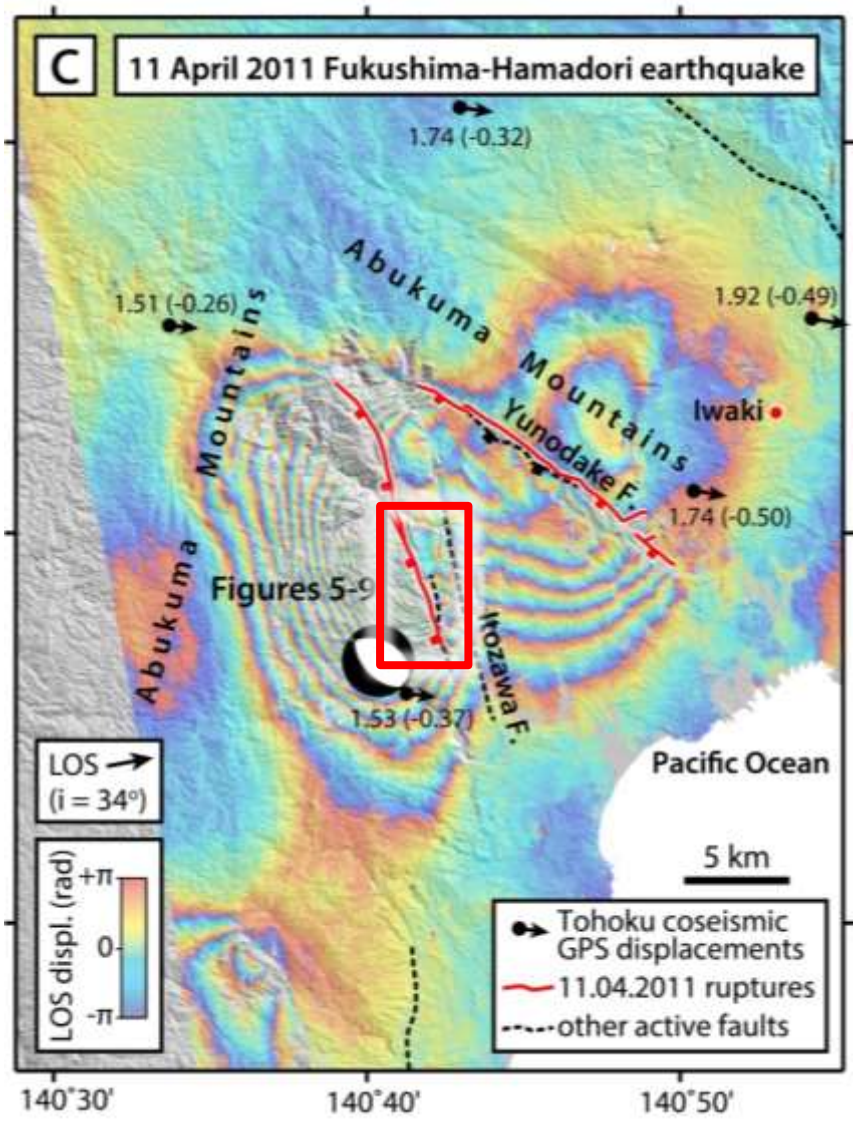

Post-event 1 m DEM

AERO ASAHI CORPORATION

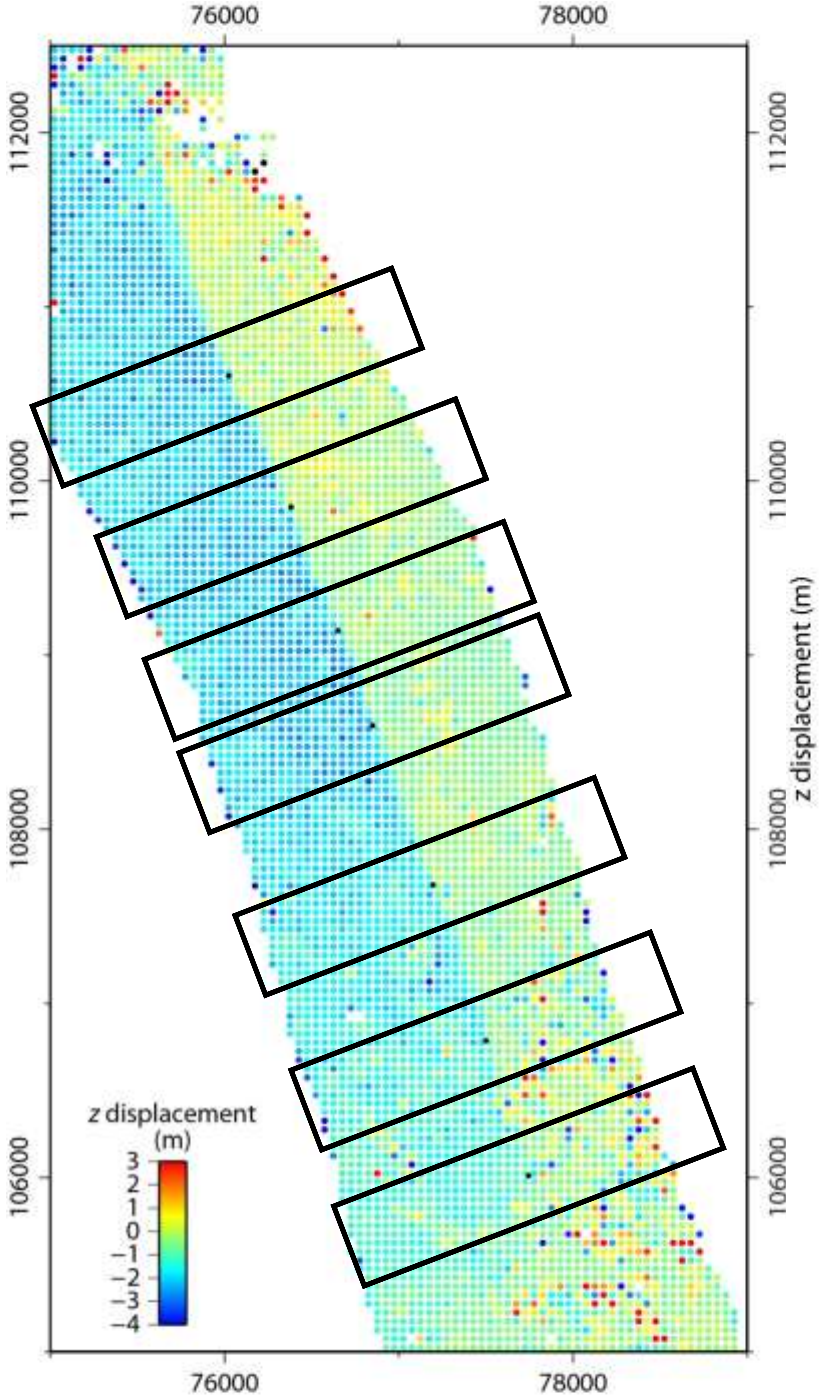

76000
78000
112000
110000
108000
106000
z displacement (m)
z displacement
(m)
3
2
1
0
−1
−2
−3
−4

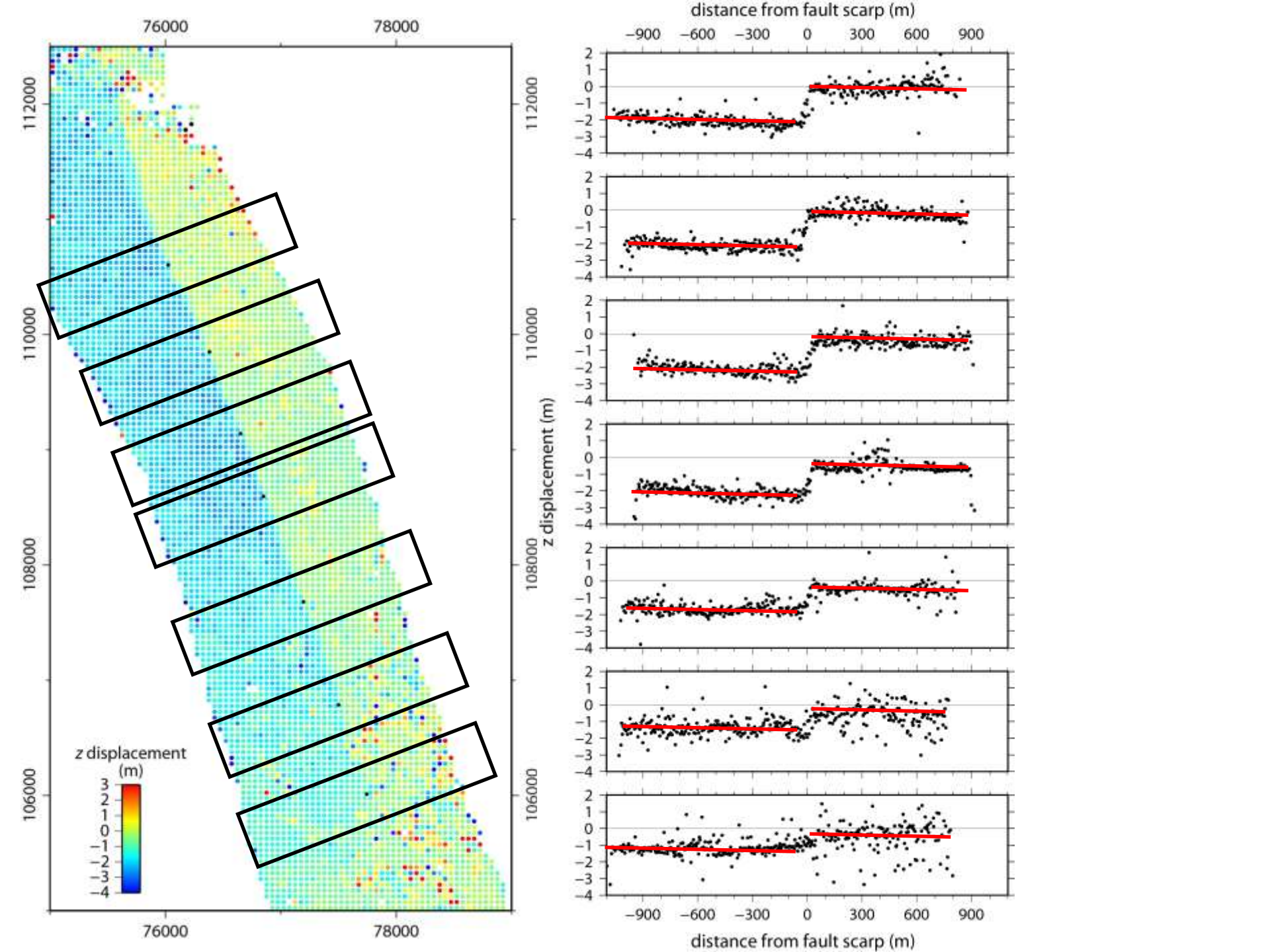
76000
78000
112000
110000
108000
106000
z displacement (m)
3
2
1
0
−1
−2
−3
−4
distance from fault scarp (m)
−900
−600
−300
0
300
600
900
z displacement (m)

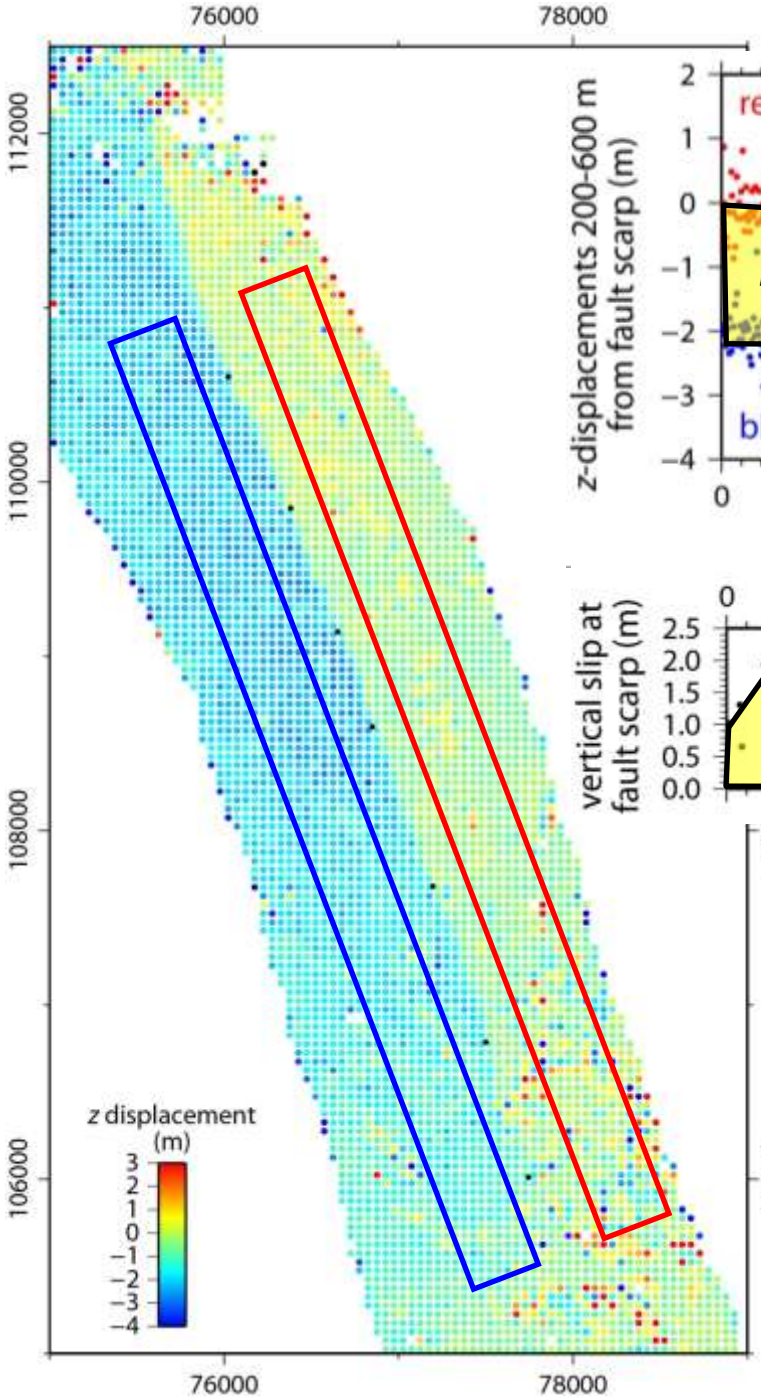

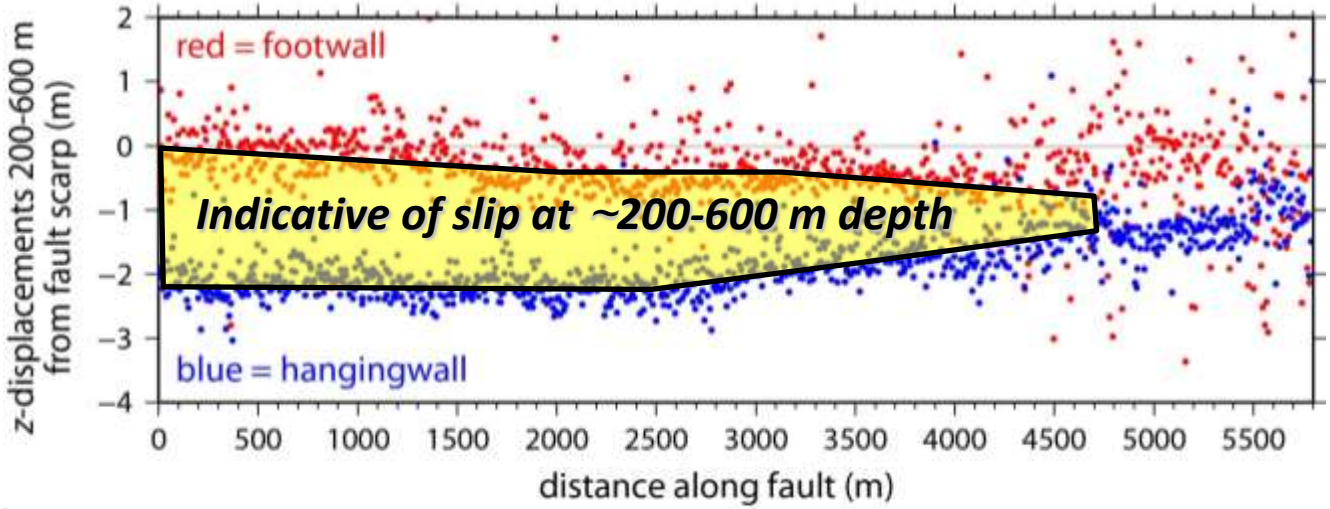

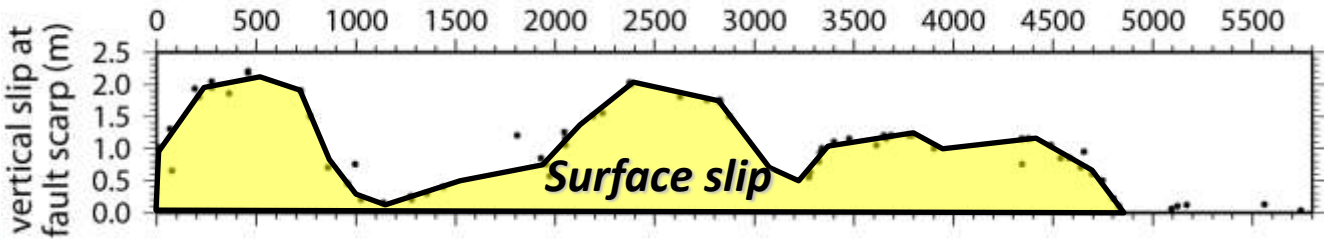

- In many places, only a small proportion of the slip makes it to the surface

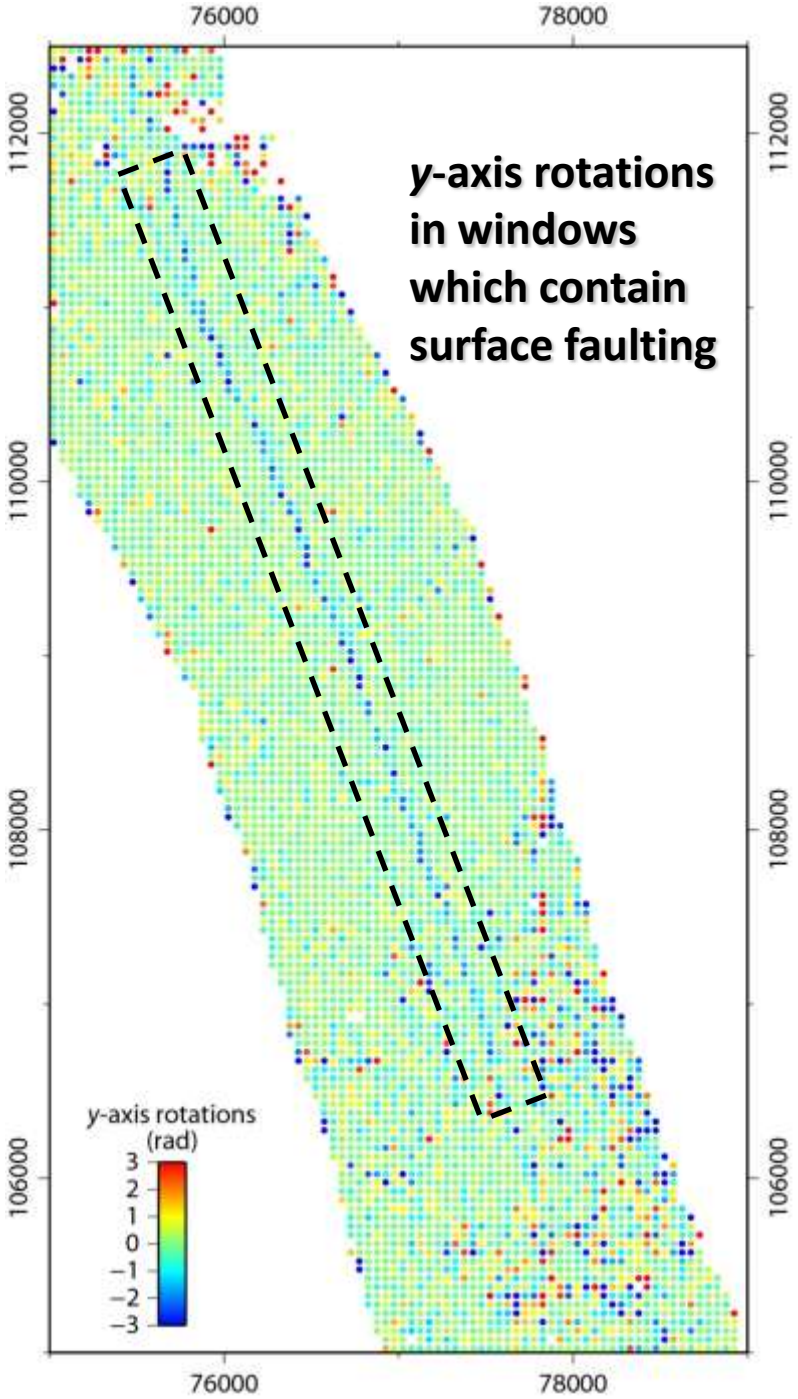
76000
78000
112000
110000
108000
106000
y-axis rotations in windows which contain surface faulting
y-axis rotations (rad)
3
2
1
0
−1
−2
−3

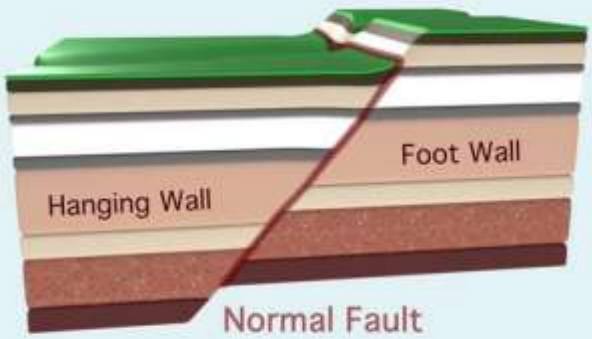
Foot Wall
Hanging Wall
Normal Fault

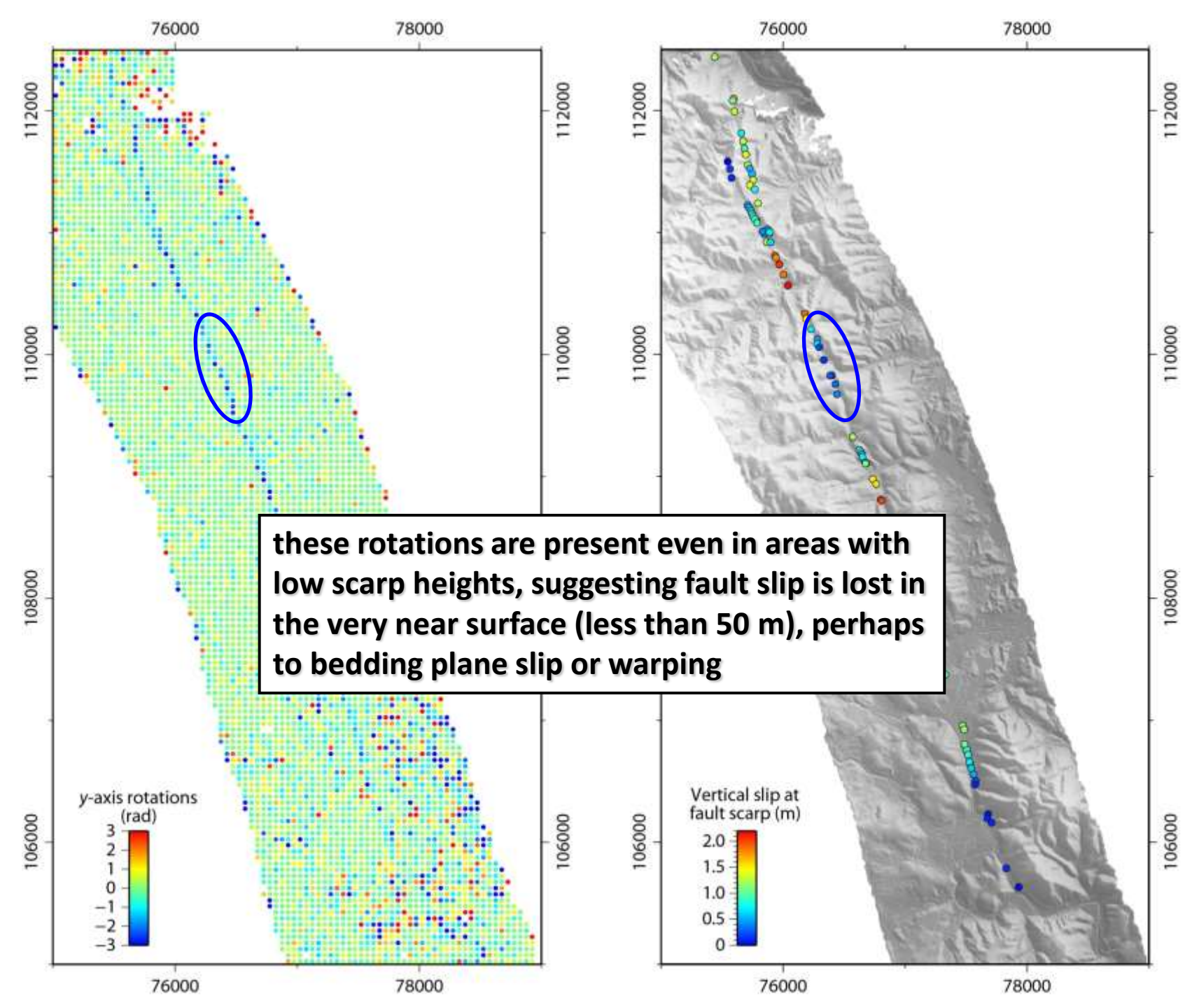
76000
78000
112000
110000
108000
106000
y-axis rotations (rad)
3
2
1
0
−1
−2
−3
these rotations are present even in areas with low scarp heights, suggesting fault slip is lost in the very near surface (less than 50 m), perhaps to bedding plane slip or warping
Vertical slip at fault scarp (m)
2.0
1.5
1.0
0.5
0

Visualizing Earth surface processes with SfM

Degradation of the 2010 El Mayor-Cucapah earthquake scarp

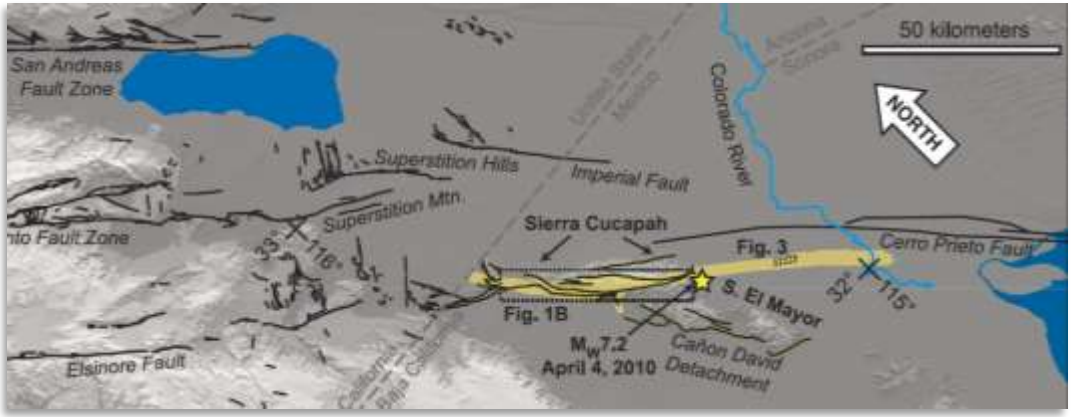

Visualizing Earth surface processes with SfM

Degradation of the 2010 El Mayor-Cucapah earthquake scarp

- ~**500 photographs** captured in about **2 hours** using a helium blimp deployed at ~100 m
- these were used to generate a ~**500 points/m^2 point cloud** and 5 cm DEM

Visualizing Earth surface processes with SfM

Degradation of the 2010 El Mayor-Cucapah earthquake scarp

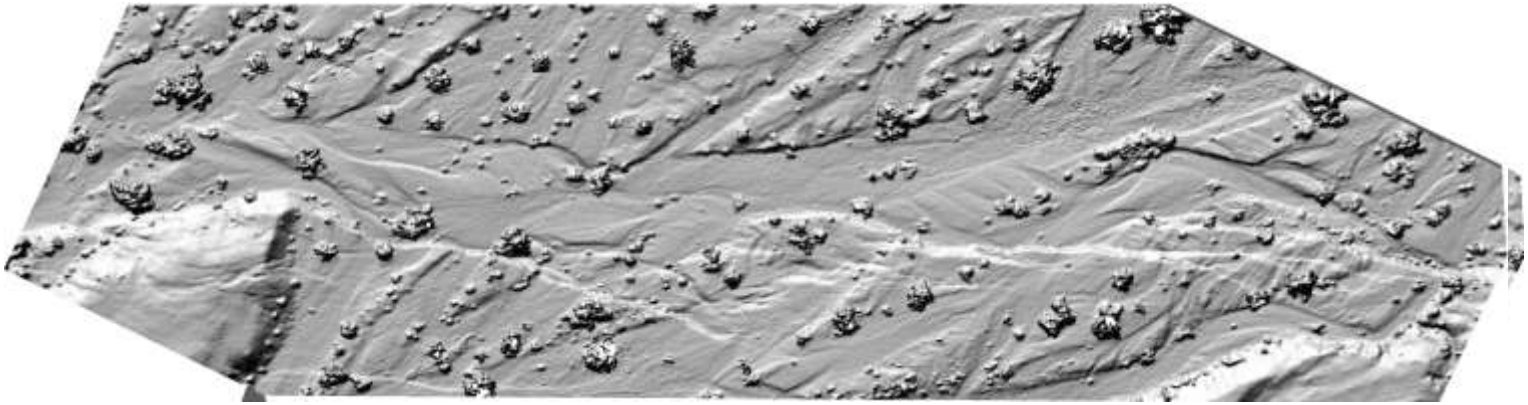

0.5 m airborne LiDAR DEM (Apr 2010)

0.05 m SfM DEM (Nov 2013)

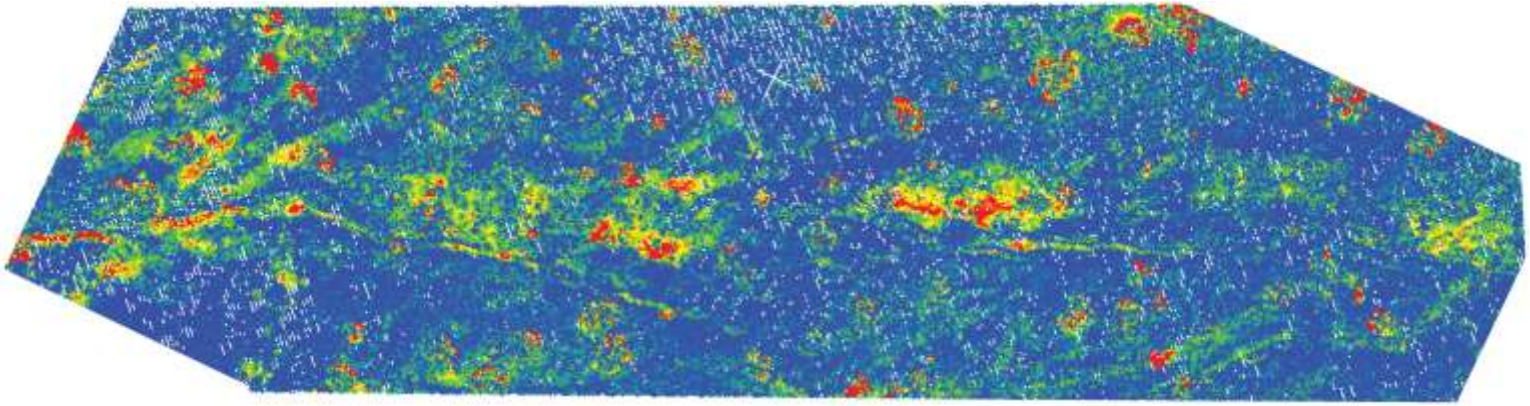

Closest point distance map (Apr 2010 - Nov 2013)

- ~**500 photographs** captured in about **2 hours** using a helium blimp deployed at ~100 m
- these were used to generate a ~**500 points/m^2 point cloud** and 5 cm DEM
- this dataset can be compared to an LiDAR survey undertaken right after the earthquake

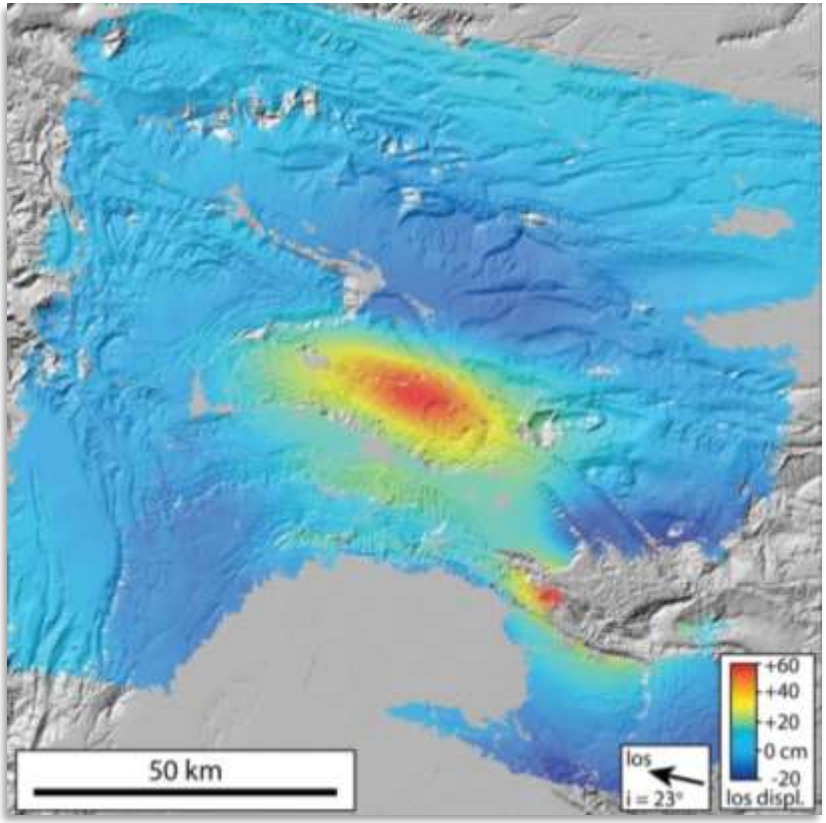

Pass 1: pre-earthquake

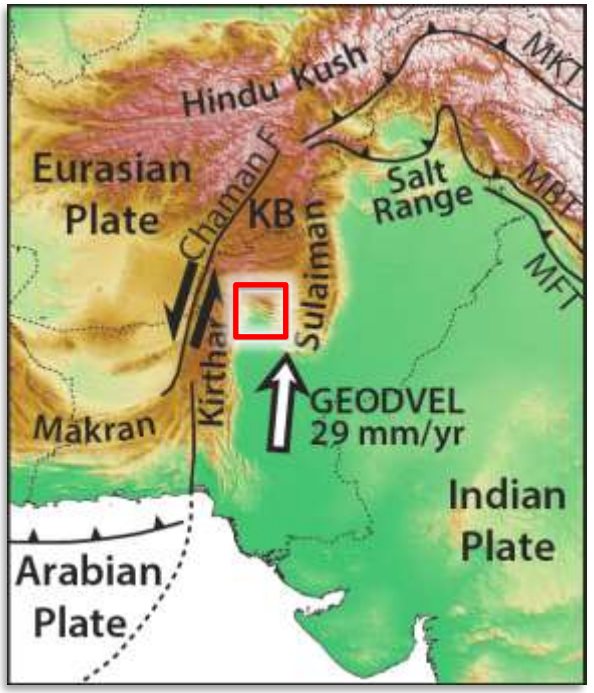

Pass 2: post-earthquake

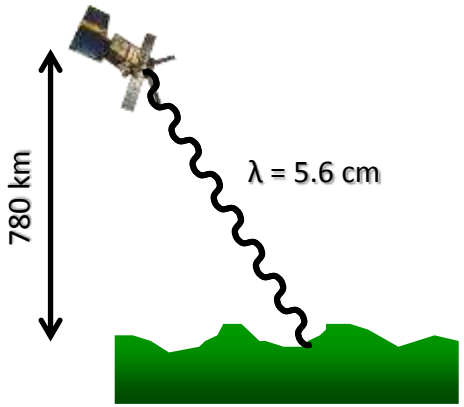

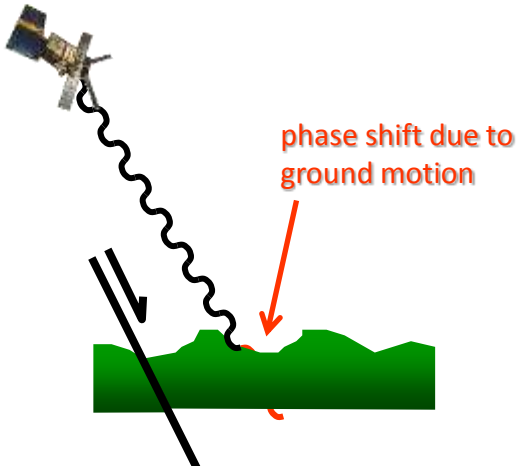

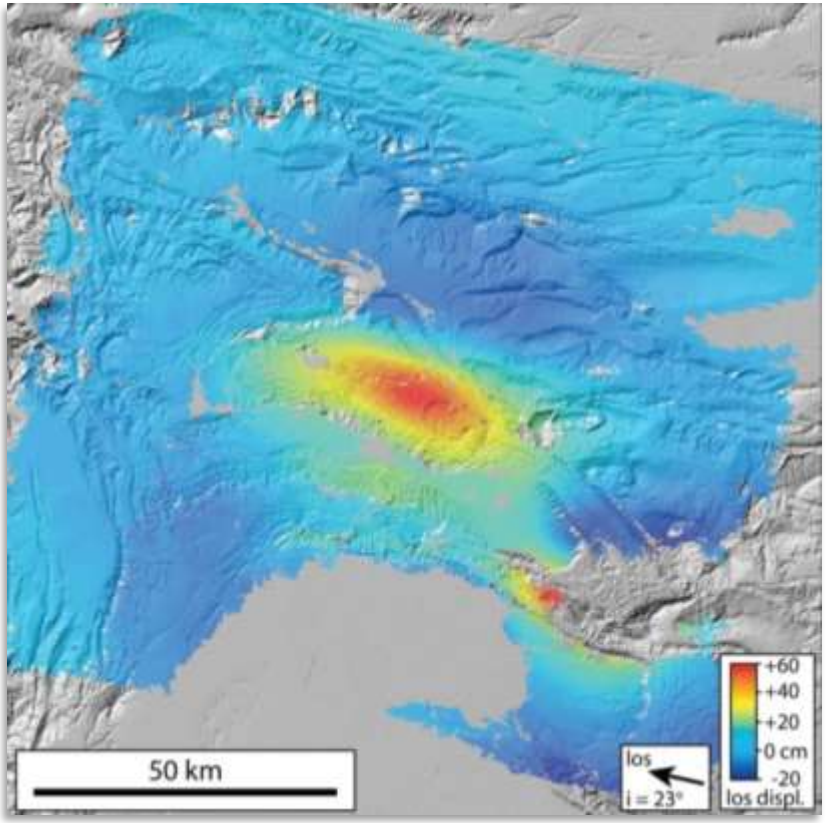

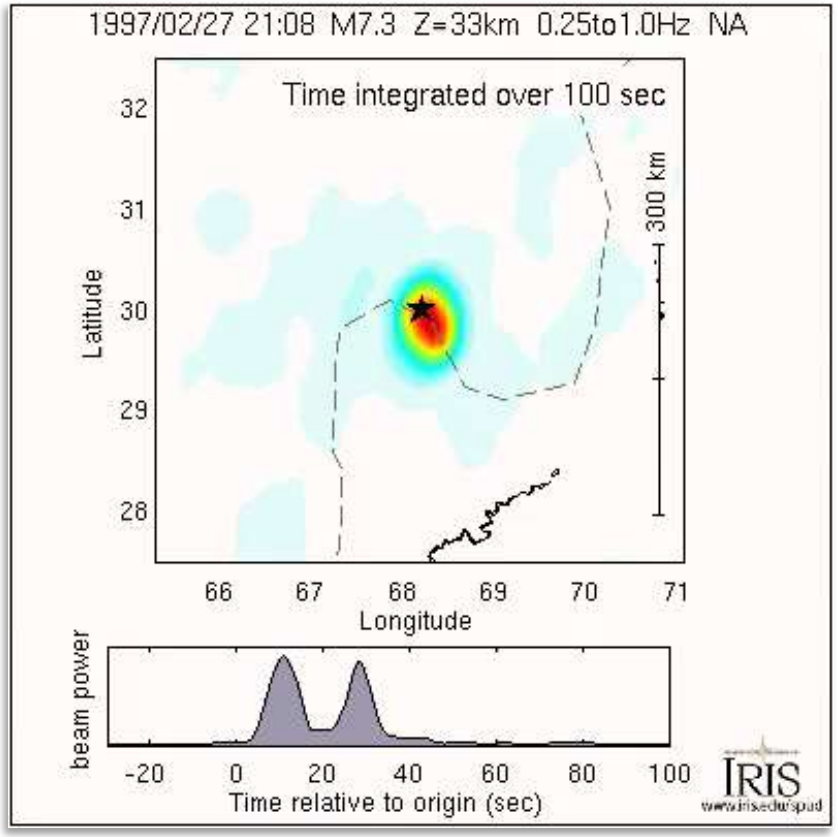

Seismic array used as "antenna"

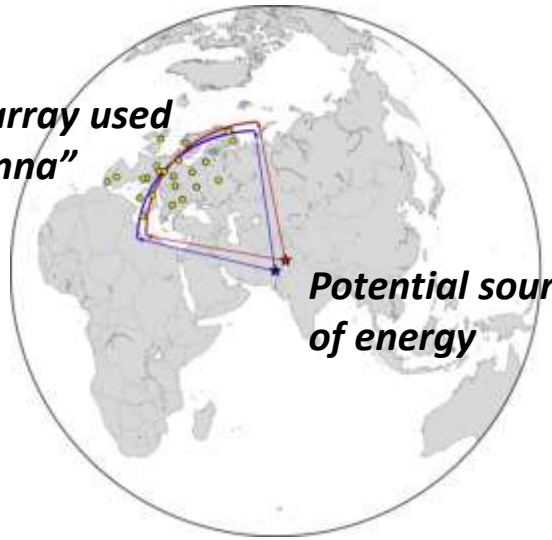

Potential sources of energy